UNIVERSIDADE DE LISBOA
FACULDADE DE CIÊNCIAS
DEPARTAMENTO DE BIOLOGIA VEGETAL

Identification and real time PCR expression analysis of drought-related lipid metabolism genes in soybean

Daniela Alves Jardim Sardinha Ferreira

Mestrado em Biologia Molecular e Genética

Dissertação orientada por:
Professora Doutora Ana Rita Matos
Doutora Andreia Figueiredo

2017

Declaração

De acordo com o disposto no artigo n.º 19 do Regulamento de Estudos de Pós – Graduação da Universidade de Lisboa, Despacho n.º 2950/2015, publicado no Diário da República, 2.ª série — N.º 57 — 23 de março de 2015, foram incluídos nesta dissertação os resultados do poster:

Ferreira, D., Duarte, B., Caçador, I., Gameiro, C., Utkin, A., Figueiredo, A., Matos, A. R. (2017). Analysis of the lipid content and photosynthesis in *Glycine max* under drought stress. 3rd COST General Meeting, Instituto de Tecnologia Química e Biológica (ITQB), Oeiras, Portugal.

Em cumprimento com o disposto no referido despacho, esclarece-se ser da minha responsabilidade a execução das experiências que estiverem na base dos resultados apresentados (exceto quando referido em contrário), assim como a interpretação e discussão dos mesmos.

Lisboa, 21 de Novembro de 2017

Daniela Alves Jardim Sardinha Ferreira

Agradecimentos

O presente trabalho foi desenvolvido no Departamento de Biologia Vegetal, no grupo Biosystems and Integrative Sciences Institute (BioISI), Faculdade de Ciências da Universidade de Lisboa, sob a orientação da Professora Doutora Ana Rita Matos e da Doutora Andreia Figueiredo.

Em primeiro lugar, gostaria de agradecer à Professora Doutora Ana Rita Matos e à Doutora Andreia Figueiredo por me concederem a oportunidade de trabalhar neste projeto. Agradeço também por tudo o que me ensinaram, pelo apoio prestado e, sobretudo, pela paciência (que eu sei que foi preciso muita).

Agradeço ao Doutor Bernardo Duarte por me ter introduzido à técnica do PAM, bem como pela ajuda que me deu em vários aspetos que me foram surgindo no decorrer do trabalho. E mais uma vez, obrigada também pela paciência.

Agradeço ao Doutor Andrei Utkin (INOV) e à Doutora Carla Gameiro pela oportunidade de trabalhar com a técnica do LIF.

Ao Professor Doutor Jorge Silva por me permitir o uso da câmara termográfica e à Professora Doutora Anabela Bernardes pela sua disponibilidade, um grande obrigado.

À Joana Figueiredo, obrigada pela ajuda na parte bioinformática e na parte de análise de dados e à Marisa Maia, obrigada pela paciência e por teres sido uma "segunda professora".

Um agradecimento aos meus amigos: Clemente da Silva, Gonçalo Laureano e Rui Nascimento pela companhia e apoio mútuo. Ao Eduardo Feijão e Miguel Gaspar, obrigada por todos os momentos em que chorámos a rir e por, ao longo deste ano, se terem tornado grandes amigos.

Um agradecimento muito, muito especial à minha amiga Manuela Lucas por ter sido a pessoa mais querida e a melhor conselheira do mundo e por ter aturado tantas vezes as nossas parvoíces.

Por fim, mas não menos importante (os últimos são sempre os primeiros), um muito obrigado aos meus pais, que são os melhores do mundo e sempre apoiaram as minhas decisões.

Abstract

Soybean (*Glycine max*) is among the most important food crops due to the high protein and lipid content of its seeds. Its importance in the world economy is not only related to its use as a food commodity but also due to its impact in the biodiesel industry.

World agriculture face major constrains with the increase of global warming, being drought a major factor affecting productivity. Soybean is considerably sensitive to drought. Previous studies have shown that the lipid content and composition of plant leaves change in response to water deficit, as a result of variations in both biosynthetic and lipolytic enzymatic activities. These changes can be related to the induction of signaling pathways, leading to the activation of drought resistance mechanisms, but can also reflect structural changes at the membrane level. Several lipolytic enzymes are involved in such processes, including phospholipases A (PLA), which remove fatty acids from membrane lipids. Despite the importance of this group of enzymes in the mediation of stress responses, revealed namely by studies using Arabidopsis, little is known about their role in drought-induced remodeling of the lipid metabolism in soybean leaves. In the present study, a comprehensive analysis of the PLA superfamily in the soybean genome allowed the identification of 50 genes, belonging to the three major plant PLA families: patatin-like phospholipases (pPLA), DAD-like phospholipase A1 (PLA1) and low molecular weight secreted phospholipase A2 (sPLA2) as well as a phosphatidic acid-preferring PLA1 (PA-preferring PLA1). Although the number of soybean PLAs is considerably higher than the one present in *Arabidopsis*, comparative sequence analyses revealed a high conservation between orthologs from the two species, which may indicate conserved functions. The expression of a subset of PLA genes, selected according to publicly available transcriptomics data and predicted subcellular location, together with other key lipid metabolism genes, was investigated by qPCR, under three stages of water deficit. Lipid profiling data revealed that the typical reduction in the plastidial lipids content was accompanied by a transient increase in linolenic-acid enriched- phosphatidylcholine and neutral lipids, suggesting a channeling of plastidial fatty acids into triacylglycerol. The potential involvement of PLA isoforms in this process is discussed, taking into account their expression profiles under water deficit, together with literature data on the subcellular locations and substrate specificities of orthologous proteins.

Since thylakoid membranes are affected by drought, some photosynthetic features were assessed, such as chlorophyll- content and fluorescence, through pulse amplitude modulation (PAM) and laser induced fluorescence (LIF) analyses. The results show variations in chlorophyll content as well as an adaptation of the photosynthetic apparatus to moderate drought, but reveal the negative impact of severe drought.

Keywords: Soybean, Phospholipase A superfamily, water deficit, gene expression, lipids profiling

Resumo alargado

A soja (*Glycine max*) é uma leguminosa amplamente consumida, cuja produção mundial compete com as dos cereais. O seu valor advém do facto de ser rica em macronutrientes, designadamente proteínas e lípidos. Os lípidos presentes apresentam importância acrescida a nível industrial, dado que por reação de transesterificação se obtêm ésteres metílicos de ácidos gordos, os constituintes do biodiesel.

As Nações Unidas estimam um crescimento da desertificação em regiões áridas, semiáridas e sub-húmidas a uma taxa de 23 hectares por minuto. Deste modo, torna-se inviável a produção agrícola, com consequências negativas nos ecossistemas, no clima, no desenvolvimento económico dos países e no bem-estar populacional. A disponibilidade hídrica tem sido considerada o fator climático de maior efeito sobre a produtividade agrícola, afetando o cultivo da soja, espécie considerada sensível à seca.

Estudos anteriores demonstraram que o conteúdo e composição lipídica das folhas são alterados em resposta ao stress hídrico. Estas alterações poderão estar relacionadas com a indução de vias de sinalização que ativam mecanismos de resistência, mas podem igualmente refletir danos membranares induzidos pelo stress. Enzimas lipolíticas, como as fosfolipases A (PLA), estão envolvidas na alteração dos lípidos de membrana. Apesar da importância destes enzimas nos mecanismos lipolíticos, o seu envolvimento na resistência ao stress hídrico ainda não está totalmente caracterizado.

No presente trabalho, pretendeu-se caracterizar os mecanismos de resposta da soja ao stress hídrico e investigar o envolvimento das fosfolipases A neste processo.

O ensaio experimental de stress hídrico consistiu na suspensão da rega de plantas em vaso, até um período máximo de 7 dias. Diferentes níveis de stress foram definidos: moderada, severa e extrema, tendo em conta o teor hídrico das folhas e do solo. Com o objetivo de estudar os efeitos do stress hídrico na composição de lípidos foliares, realizaram-se análises de cromatografia gasosa e de camada fina.

Os resultados obtidos apontam para uma acentuada diminuição do teor dos galactolípidos, monogalactosildiacilglicerol e digalactosildiacilglicerol (MGDG e DGDG, respetivamente) e um aumento do conteúdo de lípidos neutros, onde se inclui o triacilglicerol (TAG). O ácido gordo mais abundante nas membranas das folhas de soja, o ácido linolénico (C18:3) apresenta uma diminuição no MGDG e no DGDG, ao contrário do que sucede nos lípidos neutros. Visto que as membranas dos cloroplastos são ricas em galactolípidos e se observaram alterações nestes sob condições de stress hídrico, procedeu-se ao estudo do comportamento do aparelho fotossintético. Para tal, analisou-se o conteúdo clorofilino, bem como a fluorescência da clorofila, recorrendo aos métodos de fluorometria de pulso de amplitude modulado (PAM) e de fluorescência induzida por laser (LIF). Os resultados apontam para um decréscimo do rácio clorofila *a*/*b*, previamente descrito como um indicador de stress. Os dados do PAM relativos ao rendimento máximo do fotossistema II não apresentam variação, no entanto, a eficiência fotossintética da captação da luz e a taxa de transporte eletrónico máximo decresceram com a seca, indicando que o fotossistema II é relativamente resistente, mas a cadeia de transporte eletrónico é sensível aos danos causados pelo stress. Confirmando esses dados, também se verificou que, no estado mais severo de seca, existiu uma maior absorção de energia aumentando o potencial redox negativo. Uma vez que o excesso de potencial redox negativo pode causar danos no fotossistema, esta energia terá de ser libertada. Os dados do LIF apontam para uma alteração no pico de fluorescência na região do vermelho-longínquo, com uma diminuição da fluorescência máxima. Estas alterações não se prendem com a diminuição do conteúdo de clorofila a, pois este não revela diferenças, no entanto podem estar relacionadas com características estruturais e óticas das folhas de soja, nomeadamente o coeficiente de absorção e a refletância que já foram previamente descritas, em soja, como sendo baixa e alta, respetivamente.

Com o objetivo de melhor compreender as vias metabólicas associadas às alterações da composição lipídica previamente descritas procedeu-se a uma análise de expressão génica. Numa primeira abordagem caracterizou-se a superfamília das fosfolipases A (PLAs) de *Glycine max* cultivar Williams 82, cujo genoma se encontra sequenciado. A superfamília das PLA de soja é caracterizada por 50 genes que codificam 55 proteínas, distribuídos por 17 dos 20 cromossomas da planta. Esta superfamília, à semelhança de *Arabidopsis thaliana* e *Oryza sativa*, encontra-se subdividida em quatro famílias as PLA1, as com preferência para o ácido fosfatídico (PA-preferring PLA1), as PLA do tipo patatina (pPLA) e PLA2 secretadas ($sPLA_2$). As PLA1 apresentam o domínio lípase 3 e as pPLA partilham o domínio patatina. Em ambas as famílias PLA1 e pPLA verifica-se uma divisão em 3 subgrupos, I, II e III, bem como a presença dos motivos conservados GxSxG (PLA1) e GTSTG (pPLA). A família das sPLA apresenta proteínas de menor peso molecular, exibindo o motivo conservado PA2c.

Posteriormente, e de forma a comprovar a hipótese de que os ácidos gordos, com especial foco no C18:3, são libertados dos galactolípidos por ação das PLA plastidiais, sendo de seguida exportados para o citosol e incorporados no PC em condições de stress, foi avaliada a expressão de vários genes das PLAs. Visto que o PC é um intermediário na biossíntese de TAG, sendo o C18:3 incorporado neste lípido de reserva, num processo envolvendo uma PLA citosólica e/ou PDAT, foi também avaliada a expressão de 2 enzimas envolvidos na biossíntese do TAG, designadamente o Acil-CoA: Diacilglicerol Aciltransferase (DGAT) e o Fosfolípido: Diacilglicerol Aciltransferase (PDAT) que transferem um grupo acilo de modo a produzir Triacilglicerol (TAG); e uma dessaturase, a Omega-3 Dessaturase de ácidos gordos (FAD3), responsável pela conversão de C18:2 em C18:3. A análise de expressão da FAD3 foi realizada, pois o aumento de C18:3 no PC poder-se-ia dever à atividade deste enzima. Contudo, os resultados apontam para uma forte repressão do gene codificante para este enzima, em condições de seca, o que apoia a nossa hipótese a favor de uma acumulação transiente do C18:3 plastidial no PC, que é depois incorporado no TAG. Nas sementes, DGAT e PDAT estão envolvidos na biossíntese de TAG, pelo que se estudou se estes enzimas seriam ou não expressos nas folhas de soja. A análise de expressão do DGAT e do PDAT revelou que estes enzimas mantêm-se inalterado e reprimido, respetivamente, o que apoia o facto de poder haver um outro mecanismo, nas folhas, para a biossíntese de TAG, possivelmente envolvendo as PLA.

Index

Figures and tables index

Equations index

Abbreviations

ABA – Abscisic acid
ABS/CS – Absorbed energy flux per cross section
C16:0 – Palmitic acid
C16:1*t* – trans- hexadecaenoic acid
C17:0 – heptadecaenoic acid
C18:0 – Stearic acid
C18:1 – Oleic acid
C18:2 – Linoleic acid
C18:3 – Linolenic acid
cDNA – Complementary DNA
Chl *a* – Chlorophyll *a*
Chl *b* – Chlorophyll *b*
DBI – Double bond index
DAG – Diacylglycerol
DGAT – Acyl-CoA: Diacylglycerol Acyltransferase
DGDG – Digalactosyldiacylglycerol
DIo/CS – Energy dissipation as heat per cross section
DNA – Deoxyribonucleic acid
DW – Dry weight
EST – Expressed sequence tag
ETo/CS – Electron transport flux per cross section
ETC – Electron transport chain
ETR – Electron transport rate
FAD3 – Omega-3 fatty acid Desaturase
FAME – Fatty acid methyl ester
FFA – Free fatty acids
Fr/Ffr – Fluorescence red/Fluorescence far-red
Fv/Fm – Maximum yield of primary of PSII
FW – Fresh weight
GC – Gas chromatography
gDNA – Genomic DNA
H% - Water content
IP_3 – Inositol trisphosphate
LHCII – Light harvesting complex II
LIF – Laser induced fluorescence
LPCAT – Lysophosphatidylcholine acyltransferase
MDA – Malondialdehyde
MGDG – Monogalactosyldiacylglicerol
NL – Neutral lipids
PA – Phosphatidic acid
PAM – Pulse amplitude modulation
PAR – Photosynthetic active radiation
PC – Phosphatidylcholine
PDAT – Phospholipid: Diacylglycerol Acyltransferase
PE – Phosphatidylethanolamine

PG - Phosphatidylglycerol
PI – Phosphatidylinositol
PLA – Phospholipase A
pPLA – Patatin-related phospholipase A
PSI – Photosystem I
PSII – Photosystem II
Q_A – Quinone A
qPCR – quantitative polymerase chain reaction
REo/CS – Reduction energy flux per cross section
RLC – Rapid light curve
RNA – Ribonucleic acid
RWC – Relative water content
$sPLA_2$ – Secreted PLA_2
TAG – Triacylglycerol
TLC – Thin layer chromatography
TRo/CS – Trapped energy flux per cross section
TW – Turgid weight
α – Light harvesting efficiency of photosynthesis

1. Introduction

1.1 Water scarcity and its consequences in crops productivity

World agricultural production is set by three factors: increase of the world's population, limited water availability for irrigation and deterioration of arable land (Almeida *et al*., 2007). In fact, arid, semiarid and dry sub-humid regions occupy 41.3 % of land surface, and desertification is growing, mainly due to climate change. In 2030, it is projected that nearly half of the world's population will be living in areas of high water stress (United Nations, 2010).

Water is essential to all living organisms since it participates in almost all physiological and biochemical processes, being the solvent in which gases, minerals and other solutes are transported between cells. Besides, it regulates temperature and serves as mechanical support. In plants water corresponds to approximately 90 % of their total mass (Souza *et al.*, 2013).

During their life span, plants often encounter abiotic stresses such as dehydration. Abiotic stresses impose adverse growth conditions, which affect the plant development, longevity and productivity. The adaptive mechanism involves the activation of numerous signal transduction pathways, which lead to various molecular, cellular and physiological changes (Gigon *et al.*, 2004; Souza *et al.*, 2013).

In the water deficit context, the understanding and characterization of these adaptations is crucial to define sustainable strategies to cope with modern agriculture demands.

1.2 Overview on photosynthesis under drought

One of the processes that is normally impaired by drought is photosynthesis (Fig. 1) (Souza *et al*., 2013). Published data on *Citrullus lanatus* and *Lilium sp* revealed that water stress decreases photosynthetic efficiency either through stomatal effects such as lower CO_2 assimilation and/or through non-stomatal limitations like chlorophyll content decay (Sanda *et al*., 2011; Zhang *et al*., 2011). Leaf photochemistry, measured through pulse amplitude modulation (PAM) and laser induced fluorescence (LIF) is a photosynthetic assessment used earlier in many species. In *Citrullus lanatus*, hybrid Richter-110 (*Vitis berlandieri* x *Vitis rupestris*) and dark-adapted *Triticum aestivum* leaves photochemical parameters, measured by pulse modulation showed to be resistant, namely in photosystems I and II (PSI and PSII, respectively) and in electron transport rate in moderate stressed Richter-110 leaves, while in severed stress plants, electron transport rate decreases (Sanda *et al*., 2011; Flexas *et al* 2009; Lu *et al*., 1999). In contrast, greenhouse *Solanum lycopersicum*, light-adapted *Triticum aestivum* and *Olea europaea* leaves exhibit a decrease in the photochemical behavior, especially in PSII functionality (Yuan *et al*., 2015; Lu *et al*., 1999; Angelopoulos *et al*., 1996). Moreover, LIF studies in *Arabidopsis thaliana* leaves subjected to stress revealed a distinctive behavior in plants under drought stress, thus making this method an efficient alternative to PAM, with the advantage of not requiring previous dark-adaptation (Gameiro *et al*, 2016).

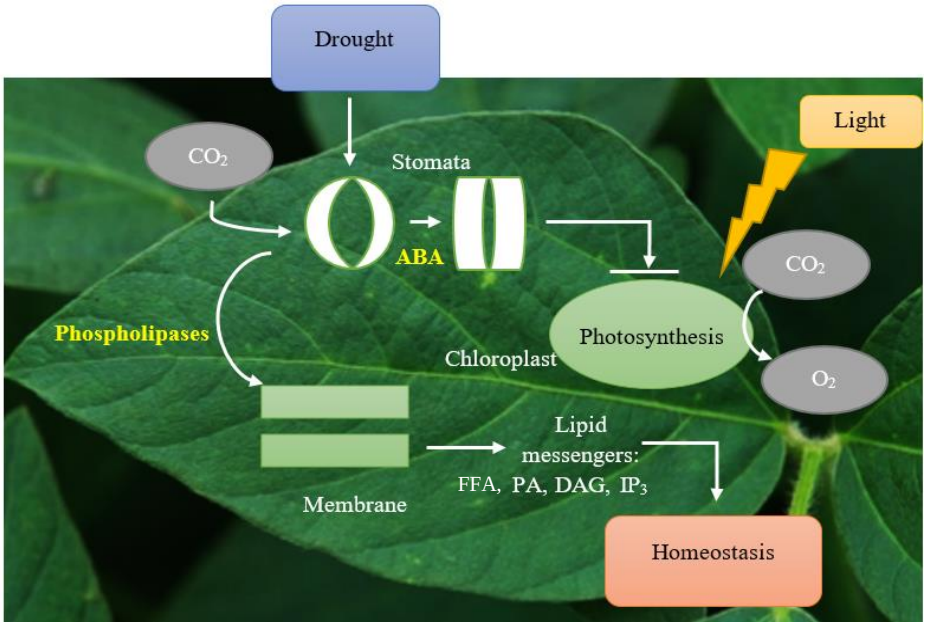

Fig. 1. Simplified illustration of plants response to drought. Stomatal response to stress, via ABA, with direct effects on photosynthesis and lipid metabolism reshaping in order for plants to return to homeostasis. ABA, abscisic acid; PA, phosphatidic acid, DAG, diacylglycerol; IP_3, inositol trisphosphate. Adapted from Osakabe *et al.*, 2014 and Zhu, 2002.

1.3 Lipids in plant cells

Recent findings propose an integral place for lipid signaling in complex regulatory network in response to abiotic stresses in plants (Singh *et al*., 2012). Various environmental cues have been identified to trigger the hydrolysis of membrane phospholipids, which results in the generation of different classes of lipid and lipid-derived signal messengers such as phosphatidic acid (PA), diacylglycerol (DAG), DAG-pyrophosphate (DGPP), lysophospholipids, free fatty acids (FFAs), phosphoinositides and inositol polyphosphates (Zhu *et al.*, 2002).

Remodeling of the membrane lipid composition has been linked to chloroplast envelope and thylakoid membranes stabilization during water stress, allowing the maintenance of chloroplasts function and photosynthetic energy supply, thus suggesting that structural re-shaping of chloroplast membranes is an essential and general mechanism of plant cellular dehydration responses (Fig. 1) (Torres-Franklin *et al*., 2007; Gasulla *et al*., 2013).

The galactolipids, monogalactosyldiacylglycerol and digalactosyldiacylglycerol (MGDG and DGDG, respectively) are the most abundant lipids in the photosynthetic membranes, constituting about 80% of thylakoid membranes (Boudière *et al.*, 2013; Páli *et al.*, 2003). Other polar lipids such as phosphatidylglycerol (PG) accounts 5-12% each for the total lipid content and phosphatidylinositol (PI) is present in low proportions of 1-5%. These polar lipids play an important role in thylakoid membranes: 1) they constitute the lipophilic matrix where PSI and PSII are located; 2) the integrity of the membrane is thought to be linked to an appropriate proportion of MGDG in a nonbilayer structure which stabilizes membrane bilayers; 3) this stability is also thought to be influenced by a small proportion of PG, that is negatively charged, which can cause repulsive forces and disruption of the membrane, if existing in great quantity; 4) they allow the existence of a certain level of membrane fluidity, which otherwise would be diminished, since thylakoid membranes exhibit a very high protein:lipid ratio; 5) galactolipids are, possibly, cofactors for complexes involved in photosynthesis, mostly PSII (Hölzl *et al.*, 2009; Härtel *et al.*, 1997; Boudière *et al.*, 2013). Besides the mentioned lipids, glycerophospholipids phosphatidylcholine (PC) and phosphatidylethanolamine (PE) are also present in plant cells, although

outside chloroplasts. Previous works have shown that PC is located in the outer envelope membrane of chloroplasts and up to 50% of total PE is located in mitochondria (Boudière *et al.*, 2013).
Storage lipids are also present in plant cells, especially in seeds, where triacylglycerol is stored in oil bodies. However, this lipid was shown to be accumulated in soybean leaves under water stress (Martin *et al.*,1986), indicating that under abiotic stress, plants response is to store lipids rich in fatty acids, in leaves, in order to face water deficit periods.

1.4 Phospholipase A superfamily response to drought

Phospholipases are of utmost importance in lipid signaling as they are essential enzymes for the catalysis of the initial step of phospholipids hydrolysis. Phospholipases have been broadly categorized as phospholipase A (PLA), phospholipase C (PLC) and phospholipase D (PLD) based on the action of respective enzyme at different sites on a glycerophospholipid molecule (Wang, 2001). PLAs form an important group of lipid hydrolyzing enzymes in plants, they can act specifically in the *sn*-1 or *sn*-2 positions, therefore, being designated PLA1 and PLA2, respectively or have a combined PLA1 and PLA2 activities, being designated PLA or lipid acyl hydrolases (for a review see Ryu 2004; Matos and Pham-Thi 2009; Chen *et al*., 2013). sPLAs are small, secreted enzymes that act in phospholipids (Matos and Pham-Thi, 2009). In fact, one Arabidopsis sPLA, *AtsPLA2-α* have showed to prefer zwitterionic phospholipids as substrate, but no activity toward anionic phospholipids, such as PG and PI was registered (Mansfeld and Ulbrich-Hofmann et al., 2007). In *Oryza sativa*, three isoforms were previously reported (Singh *et al*., 2012). In the soybean genome five isoforms were already identified by Mariani and co-workers (2012) and the activity of one recombinant isoform studied. Recently two sPLA2 were identified in the flax genome (Gupta *et al*., 2017).
A group of PLA having preference for the *sn*-1 position of phospholipids, namely PC, here designated PLA1, are related to fungal lipases and can also act on triacylglycerol (Richmond *et al*., 2011). In *Arabidopsis thaliana* and *Oryza sativa*, they include subfamilies I, II and III with, respectively 7, 4 and 1 isoforms identified for Arabidopsis (Ishiguro *et al*., 2001), while in *Oryza sativa* genome only group I (8 isoforms) and II (3 isoforms) were identified (Singh *et al*., 2012).
Patatin-like PLA have a broad substrate specificity, including both phospholipids and galactolipids and are able to act on both *sn*-1 and *sn*-2 positions (Matos *et al*., 2001; Matos *et al*., 2008; Scherer *et al*., 2010). pPLAs comprise three subfamilies (I, II and III), with respectively, 1, 5 and 4 genes in Arabidopsis (Holk *et al*., 2002) and 1, 9 and 6 genes in *Oryza sativa* (Singh *et al*., 2012). In Arabidopsis, Matos and co-workers (2008) have showed that pPLA-IIα acts on phosphor and glycolipids, with preferences as follows: PG>PC>MGDG>DGDG. The up-regulation of a pPLA (*VuPAT1*) under drought conditions was firstly reported by our group in the leaves of the tropical legume *Vigna unguiculata* (Matos *et al*., 2001). The study of the enzymatic activity of the recombinant protein revealed that it encoded an enzyme able to release fatty acids from galactolipids. However, the lack of genome sequence in this legume hampered a more detailed analysis of other drought regulated PLAs. Further work allowed the identification of other two group II and one group III pPLA genes in Arabidopsis (Matos *et al*., 2008), up-regulated by drought in parallel with a decrease in the plastidial lipids and an increase in the relative amounts of free polyunsaturated fatty acids as well as neutral lipids (Gigon *et al*., 2004; Matos *et al*., 2008). In *Oryza sativa* seedlings, Singh *et al*. (2012) reported up-regulation of a patatin-like gene, *OspPLA-IIIa*, under drought conditions. Besides patatins, PLAs belonging to other groups were shown to have their expression increased under water deficit. In *Triticum durum*, three transcripts of sPLA were shown to accumulate under water deficit, *TdsPLA2I*, *TdsPLA2III* and *TdsPLA2IV* (Verlotta *et al*., 2013). Also, the involvement of DAD1-like lipases in response to salt and osmotic stress was observed in Arabidopsis (Ellinger and Kubigsteltig *et al*., 2010).

1.5 *Glycine max* under drought

Soybean is ranked among the most important agriculture food crop, even competing with cereals like corn and wheat. In fact, soybean worldwide production increased from 161 million tons in 2000 to 306 million tons in 2014 (Martynenko *et al.*, 2016; FAOSTAT, 2016). Soybean is highly rich in macronutrients such as proteins (40%) and lipids (20%) (Souza *et al.*, 2013) being an elite crop for both human food and animal feed. Moreover, the lipid content of soybean makes this crop very important for biodiesel production (USDA, 2017). Sustainability of soybean yields is, however, threatened by predicted climatic changes with persistent droughts over many parts of the world.

During development, soybeans are very vulnerable to drought. Previous studies have shown that in the third week of plants' growth, 4 days of stress results in 36% loss (Martynenko *et al*., 2016). Also in adult plants, and mainly during the flowering stage, in which water need peaks (Souza *et al*., 2013), these stress conditions trigger a chain of physiological responses starting in plant leaves and going from morphological and structural adaptation (Bacelar *et al*., 2004) to hormone regulation (Peleg *et al*., 2011) in order to maintain homeostasis (Morgan, 1984).

Moreover, stress conditions cause losses in CO_2 assimilation, decrease in leaf area, decrease in size and number of pods and affects negatively the symbiotic nitrogen fixation, due to accumulation of ureides (nitrogen products) which cause feedback inhibition of N_2 fixation (Purcell et al., 1999; Sinclair et al., 2007). Furthermore, abscisic acid signaling takes action, causing stomata closure, which increases leaves' temperature. Leaf abscission occurs due to ethylene's enhanced synthesis and roots grow in order to reach deeper humid zones in the soil. This happens because of a shift in mobilizing carbon sources from the development of the leaf to the growth of the root (Akýnci *et al*., 2012).

Lipid content is also affected in *Glycine max*. In fact, Martin and co-workers (1986) have studied glycerolipid response to water stress. They observed that galactolipids fraction and PG varied little during drought treatment, whereas PA, PI and PC increased in *Glycine max* leaves.

Despite all the advances on the characterization of drought related mechanisms in soybean, little is known on the lipid modulation under water deficit.

2. Aim

The aim of this work was to characterize lipid modulation in soybean under water deficit. Thus, we have first evaluated photosynthetic modulation in different stages of water deficit, imposed by measuring pigment content and chlorophyll fluorescence as thylakoid membranes are main targets of drought stress. A lipid profiling by Gas Chromatography (GC) and Thin Layer Chromatography (TLC) was also performed. In order to identify drought-induced PLA that may be involved in membrane remodeling in soybean leaves, we have characterized, for the first time, the soybean phospholipase A superfamily and defined groups based on phylogenetical analyses, gene and protein primary structure. A subset of PLA genes was selected to expression analysis, according to publicly available transcriptomic data, as well as subcellular prediction, under different stages of drought conditions, in order to distinguish between primary signaling, adaptation and harmful consequences. Moreover, the expression of other key lipid metabolism genes involved in fatty acid desaturation and triacylglycerol biosynthesis was also analyzed in order to provide a comprehensive analysis of soybean leaves lipid metabolism remodeling under water deficit. The identified candidate genes could be further used in improvement soybean programs through conventional breeding or genetic transformation.

3. Material and Methods

3.1. Plant Material and Experimental Design

Surface sterilized, soybean (*Glycine max* [L.] Merr.) seeds of cv Williams 82, kindly provided by Dr Randy Shoemaker (USDA¸ Iowa State University) were grown in a phytoclimate chamber (5.000 EH ARALAB®) with the following parameters: 25-18 ºC (day-night temperatures), 50 % of relative air humidity, photoperiod of 16-8 h (day/night) and 396 μmol m^{-2} s^{-1} of photosynthetically active radiation. Plants were grown in pots containing 200 mL of soil Compo Sana Universal enriched with agrosil and perlite, 200 mL of vermiculite on top of 125 mL of lightweight expanded clay aggregate (LECA). Seedlings were watered every other day with distilled water and a nutrient solution was supplied every other week (KB Universal Liquid Fertilizer with oligoelements and 6% N, 3% $O_{10}P_4$ and 6% K_2O).
One and a half month old plants were used for the drought stress experiment. Water stress was imposed by withholding watering for a maximum of 7 days. Drought stress was monitored by pot weighting and visual inspection. One foliole of each plant was used to determine the fresh weight (FW), turgid weight (24 h floating in water in the dark at room temperature) and dry weight (DW, dry at 65 ºC until constant weight, ~48 h), in order to calculate leaf water content (H %) and relative water content (RWC) as follows:

$$3.1.\ H\% = (FW - DW)/FW \times 100$$

$$3.2.\ RWC = (FW - DW)/(TW - DW) \times 100$$

Between 10 and 17 biological were used for each type of stress. The first and second fully expanded trifoliate leaf of each plant were sampled, at the same hour of the day (2 – 3 h into the beginning of the light period) immediately frozen in liquid nitrogen and stored at – 80˚C.

3.2 Thermal imaging

Thermal screenshots were taken using a FLIR® E50bx camera (Inframetrics, FLIR Systems Inc, OR, US). Screenshots were taken at 2nd, 3rd and 6th days after withholding watering.

3.3 LIF Analysis

LIF spectrum was obtained as previously described (Gameiro *et al*., 2016). It was used a frequency-doubled Nd:YAG laser, manufactured by Quantel (model Ultra 532 30 20HN) and a LIF detector on top of Ocean Optics USB4000 spectrometer. The laser, located 1 m from the sample, provides a 30 mJ, 7 ns radiation pulses at 532 nm, with a repetition rate of 20 Hz and a spot diameter at the sample location of approximately 3 mm. The pulse radiation is maintained sufficiently low to avoid reaction centre closure and excitation annihilation. Part of the reflected fluorescence emitted is collected by a light gathering optical train based on low cost components provided by Thorlabs, assembled within the 2.54 cm diameter lens mounting tube SM1L30. The train comprises an optical filter and a telescopic system, positioned and centred using three retaining rings SM1RR. The long pass optical filter FEL0550, with the cut off wavelength of 550 nm and transmission of approximately 80% in the region of 650-730 nm, protects the spectrometer from strong retroreflected laser light. The SMA fiber optics collimation package F810SMA 635 is installed immediately after the filter. Usually being intended for collimating a laser beam propagating from the tip of an SMA-connectorized fiber, collecting the fluorescence radiation over a 21 mm diameter input pupil and transmits it into an optical fiber. This fiber transports the optical signal to the spectrometer optical bench, the USB4000-f/4 asymmetrical crossed Czerny Turner configuration with the diffraction grating Ocean Optics #9, providing nearly uniform efficiency at wavelengths from 450 to 800 nm. The spectrometer was tuned and calibrated with the help of the mercury argon calibration source CAL 2000, demonstrating the sensitivity of approximately 55 photons per count, and resolution of 0.19 nm per channel in the spectral range of interest (650 – 730 nm).

3.4 PAM fluorometry

Modulated chlorophyll fluorescence was measured as previously reported (Duarte *et al*. 2013), using FluorPen FP100 PAM (Photo System Instruments, Czech Republic). Leaves were dark adapted for 15 minutes in order to perform rapid light curves (RLC) measurements, using the pre-programmed LC1 protocol. Each ΦPSII measurement was used to calculate the electron transport rate (ETR) through photosystem II using the following equation: ETR = ΦPSII x PAR x 0.5, where PAR is the actinic photosynthetically active radiation generated by FluorPen and 0,5 assumes that the photons absorbed are equally partitioned between PSII and PSI. ETRs and the irradiance pulses from 0 to 500 μmol m^{-2} s^{-1} allowed us to obtain rapid light curves. RLC slope (α) is a measure of the light harvesting efficiency of photosynthesis and the asymptote of the curve is the maximum rate of photosynthesis which quantifies the capacity of the photosystems to use the absorbed light energy.

Kautsky induction curves, or OJIP curves, are obtained when dark adapted leaves are illuminated with the saturating light intensity of 3500 μmol m^{-2} s^{-1}, resulting in a polyphasic rise in fluorescence. These phases are OJIP, in which O stands for the open reaction centres at the onset of illumination with no reduction of QA (the stable primary electron acceptor of PSII). Between O to J, there is a net photochemical reduction of QA. From J to I all the phase represents all reduced states of closes reaction centres. P reflects the maximum concentration of reduced QA as well as the balance between incident light at the PS II, the rate of chemical energy used and the rate of heat dissipation. From this Kautsky curve we can extrapolate photochemical parameters such as the maximum yield of primary photochemistry of PSII (Fv/Fm), the absorbed energy flux per cross section (ABS/CS), the trapped energy flux per cross section (TRo/CS), the electron transport flux per cross section (ETo/CS), the reduction energy flux per cross section (REo/CS) and the energy dissipation as heat per cross section (DIo/CS).

3.5 Pigment quantification

Chlorophyll *a* and *b* content was measured as described by Lichtenthaler (1987). Pure methanol was added to leaf discs of 0.9 cm of diameter and extraction occurred at 4º C for 48 h, in the dark. The absorbances were read at 665.2 and 652.4 nm. The concentrations of pigments (μg/mL) were calculated as follows:

$$3.3.\ \text{Chl } a = 16.72 \times A_{665.2} - 9.16 \times A_{652.4}$$

$$3.4.\ \text{Chl } b = 34.09 \times A_{652.4} - 15.28 \times A_{665.2}$$

3.6 Total Lipid Extraction and Analysis

After inactivation of lipolytic activities in boiling water for 5 min, and leaf homogenization with a mortar and pestle, lipids were extracted with methanol, chloroform and water (1: 1: 1; v/v/v). After centrifugation, 3000 x g for 5 min, the lower phase was rescued and the solvent evaporated under a nitrogen stream at 37 ºC (Matos *et al*., 2008). Lipid classes were separated by thin layer chromatography using silica gel plates (G-60, Merck, Darmstadt, German) as previously described (Gigon *et al*. 2004; Esquível *et al*., 2017) using a solvent system that separates the different polar lipids, while the neutral lipids migrate at the solvent front (Matos *et al*., 2008). After visualization with primuline (0.01 % in 80 % acetone; v/v), lipid bands were scraped off and the fatty acids were methylated in methanol sulphuric acid (2.5 %). Fatty acids methyl esters (FAMEs) were separated in a gas chromatograph (Varian 430-GC gas chromatograph) equipped with a hydrogen flame ionization detector set at 300 °C. The temperature of the injector was set to 270 °C, with a split ratio of 50. The fused-silica capillary column (50 m x 0.25 mm; WCOT Fused Silica, CP-Sil 88 for FAME; Varian) was maintained at a constant nitrogen flow of 2.0 mL/min and the oven temperature set at 190 °C. Fatty acids were identified by

comparison of their retention times with standards (Sigma-Aldrich) and chromatograms analyzed by the peak surface method, using the Galaxy software. Quantitative analysis of fatty acid methyl esters was carried out using methyl heptadecanoate (C17:0) as an internal standard. The DBI (double bond index) was calculated as follows:

3.5. DBI = 2 x (1 x % monodienoic acids) + (2 x % dienoic acids) + (3 x % trienoic acids) / 100

Quantification of the lipid peroxidation products was performed as described previously (Heath *et al*., 1968). Briefly, grinded leaves were homogenized in 0.5% (w/v) of thiobarbituric acid and 20% of trichloroacetic acid and incubated for 30 minutes at 95 °C. The reaction was stopped in ice. Absorbance values at 532 nm and 600 nm (Unicam 500β UV/Vis Spectrometer, Unicam, Cambridge, UK) were registered and the concentration of TBARS calculated using the malondialdehyde (MDA) molar extinction coefficient, 155 mM^{-1} cm^{-1} (Heath *et al*, 1968).

3.6. $A_{532} - A_{600}$ = [MDA] x ε [MDA]

3.7 Identification and retrieval of *Glycine max* PLA Sequences

Phospholipases A genes and amino acid sequence identification was performed using *Arabidopsis thaliana* PLA proteins sequences (Ryu, 2004) as a query for blast searches against *Glycine max* genome in both Phytozome (https://phytozome.jgi.doe.gov/pz/portal.html) and National Center for Biotechnology Information (NCBI) (https://www.ncbi.nlm.nih.gov/) databases (August, 2017).

3.8 Domain Structure Analysis, Sequence Properties, Subcellular Location Prediction and Chromosomal location

Domain determination was performed using Pfam (http://pfam.xfam.org/). Molecular weight (Mw) and theoretical isoelectric point (pI) were predicted using the ProtParam tool from ExPASy (Gasteiger *et al.*, 2005; http://web.expasy.org/protparam/). Subcellular location of proteins was predicted using WoLF PSORT (https://www.genscript.com/wolf-psort.html) and TargetP v1.1 (http://www.cbs.dtu.dk/services/TargetP/). The Map Viewer tool from NCBI (http://www.ncbi.nlm.nih.gov/mapview/) was used to map PLA genes in *Glycine max* chromosomes.

3.9 Protein Sequence Alignment and Phylogenetic Analysis

Glycine max and Arabidopsis PLA protein sequences were aligned with Clustal W method with the MegAlign tool, included in the DNASTAR software (https://www.dnastar.com/) and soybean sequences were edited with Jalview software (http://www.jalview.org/). A maximum likelihood (ML) phylogenetic analysis was generated by BioNJ algorithm (Gascuel, 1997), a variant of the Neighbor-Joining algorithm, with Kimura method used to calculate distance values and bootstrap with 1000 iterations. Trees were viewed on FIGTree (http://tree.bio.ed.ac.uk/software/figtree/) and edited on Inkscape (http://www.inkscape.org/). Intron-exon analysis was performed using NCBI database (https://www.ncbi.nlm.nih.gov/). Using UniGene tool from NCBI (https://www.ncbi.nlm.nih.gov/unigene), expressed sequence tags (EST) were identified.

3.10 RNA Extraction and cDNA Synthesis

Total RNA was isolated from frozen leaves with the Spectrum™ Plant Total RNA Kit (Sigma-Aldrich, USA), according to manufacturer's instructions. Residual genomic DNA was digested with DNase I (On-Column DNase I Digestion Set, Sigma-Aldrich, USA). RNA purity and concentration were measured at 260/280 nm using a spectrophotometer (NanoDrop-1000, Thermo Scientific) while RNA integrity was verified by agarose gel electrophoresis (1.2% agarose in TBE buffer). Genomic DNA

(gDNA) contamination was checked by qPCR analysis of a target on the crude RNA (Vandesompele *et al.*, 2002). Complementary DNA (cDNA) was synthesized from 2.5 µg of total RNA using RevertAid®H Minus Reverse Transcriptase (Fermentas, Ontario, Canada) anchored with Oligo(dT)23 primer (Fermentas, Ontario, Canada), according to manufacturer's instructions.

3.11 Quantitative Real Time PCR

For the expression analysis, *Glycine max* PLA genes were searched in microarray data of soybean leaf tissues under drought stress (Le *et al.*, 2012) to select drought responsive PLAs. DGAT, PDAT and FAD3 gene sequences were also included in gene expression analysis (Supplementary data 1).
Quantitative real time PCR (qPCR) experiments were carried out using Maxima™ SYBR Green qPCR Master Mix (2×) kit (Fermentas, Ontario, Canada) in a StepOne™ Real-Time PCR system (Applied Biosystems, Sourceforge, USA). A final concentration of 2.5 mM $MgCl_2$ and 0.2 µM of each primer were used in 25 µL volume reactions, together with 4 µL of cDNA as template. Primer sequences and reaction details are provided in Supplementary data 1.
Thermal cycling for all genes started with a denaturation step at 95 °C for 10 minutes followed by 40 cycles of denaturation at 95 °C for 15 seconds and annealing/extension for 30 seconds. Each set of reactions included a control without cDNA template. Dissociation curves were used to analyze non-specific PCR products (Supplementary data 3). Three biological replicates and two technical replicates were used for each sample. *Golgin-84* (Glyma.08G053300.1) and *NUDIX* (Glyma.13G171900.1) were used as reference genes as previously described (Marcolino-Gomes *et al.*, 2015). Gene expression (fold change) was calculated as described in Hellemans *et al.*, (2007).

3.12 Statistical Analysis

Mann-Whitney test was performed using the software IBM® SPSS® Statistics, version 23 (SPSS Inc., USA). This is a non-parametric test, suitable for independent groups and for small sample sizes ($n < 20$). Results yielding $p \leq 0.05$ were considered statistically significant.

4. Results

4.1. Leaves hydration level and relative water content during the drought treatment

Both RWC and H% parameters were calculated for each plant, in order to define drought stress levels (Fig. 2). Plants were then grouped in moderate (S1), severe (S2) and extreme (S3) stress classes with average values 85.0, 58.9 and 38.4, respectively, for RWC and 80.1, 74.9 and 66.9, respectively for H% (Fig. 2.). Controls presented a mean RWC of 84.8 and a H% mean of 78.7, which were, approximately, the values found in S1, therefore, stomata closure and soil weight were used to distinguish the two groups. Hence, control plants had a soil weight higher than 800 g, and in moderate stressed plants, soil weight ranged from 395 to 400 g, in severe stressed plants, soil weight was 377 – 405 g and in extreme stress, soil weight was 345 – 367 g.

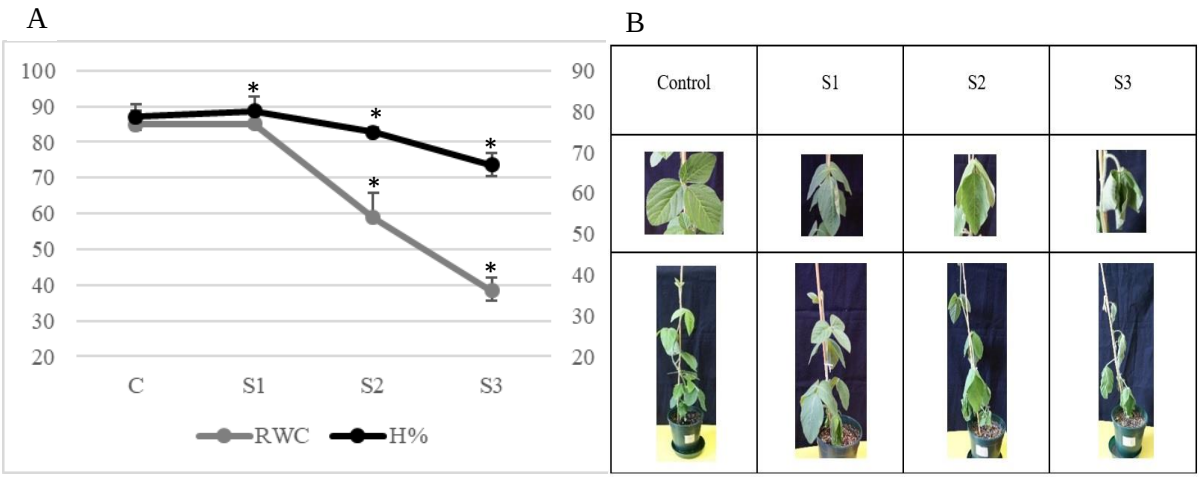

Fig. 2. Dehydration of *Glycine max* plants. (A) Relative water content (RWC %) and hydration level (H %) of *Glycine max* leaves over the course of drought treatment. C, control leaves with RWC > 71 % and H % > 78 %; S1, moderate stressed leaves with RWC > 71 % and H % > 78 %; S2, severe stressed leaves with RWC = [50 - 70] % and H % = [70 - 77] %; S3, extreme stressed leaves with RWC = [30 - 49] %; H% = [60 - 69] %. Average values ± standard deviation is shown; (B) *Glycine max* phenotype under water stress.

4.2. Thermal shifts of *Glycine max* leaves under drought

Typical appearance of control and water stressed *Glycine max* leaf tissue at the onset of water stress is shown in Fig. 3. It is possible to observe that leaves temperature increased at the 3rd day, indicating that stomata were closed and remained closed in the following days. Thus, this assay was useful to determine moderate stressed plants, since RWC (%) parameter in S1 did not vary much from the control group.

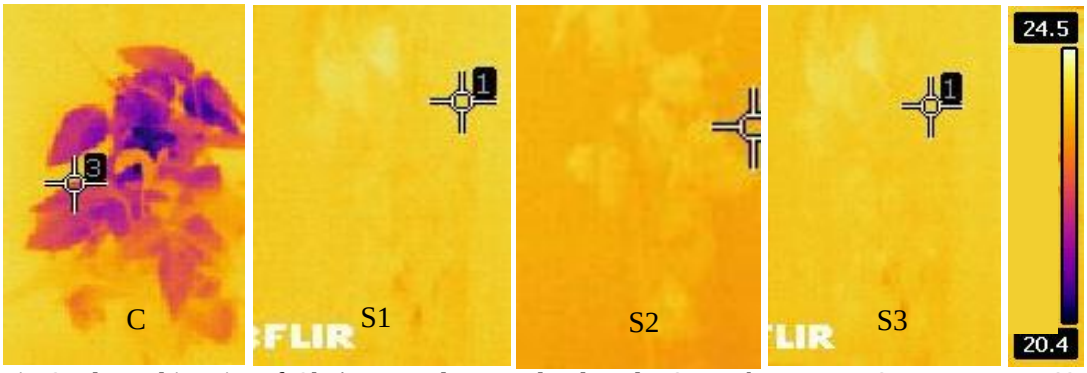

Fig. 3. Thermal imaging of *Glycine max* plants, under drought. S1, moderate stress; S2, severe stress; S3, extreme stress; C, control. Temperature scale in ºC is represented at the right of the figure.

4.3 Laser Induced chlorophyll fluorescence in *Glycine max* under drought

Maximum chlorophyll fluorescence was analyzed using LIF technology (Fig. 4). Under drought stress, this parameter tends do decrease but a significant difference, comparing to controls is observed only at S2 and S3, being both values identical (Fig. 5A).

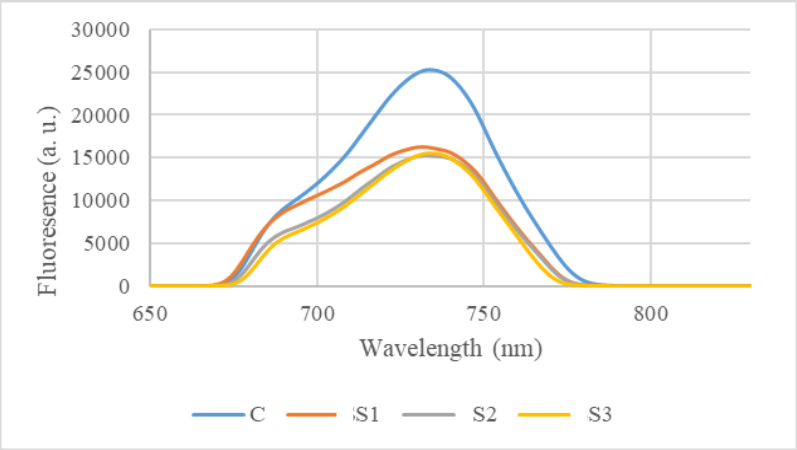

Fig. 4. Representative fluorescence spectra of *Glycine max* leaves under drought. C, control; S1, moderate stress; S2, severe stress; S3, extreme stress.

The wavelength at which maximum fluorescence occurs remains unchanged in stress treatment (Fig. 5B). When comparing the fluorescence occurring in the red- and in the far-red regions, through the Fr/Ffr, there is a tendency for a transient increase at S1 followed by a decreasing trend at S2 and S3, but not statistically significant (Fig. 5C).

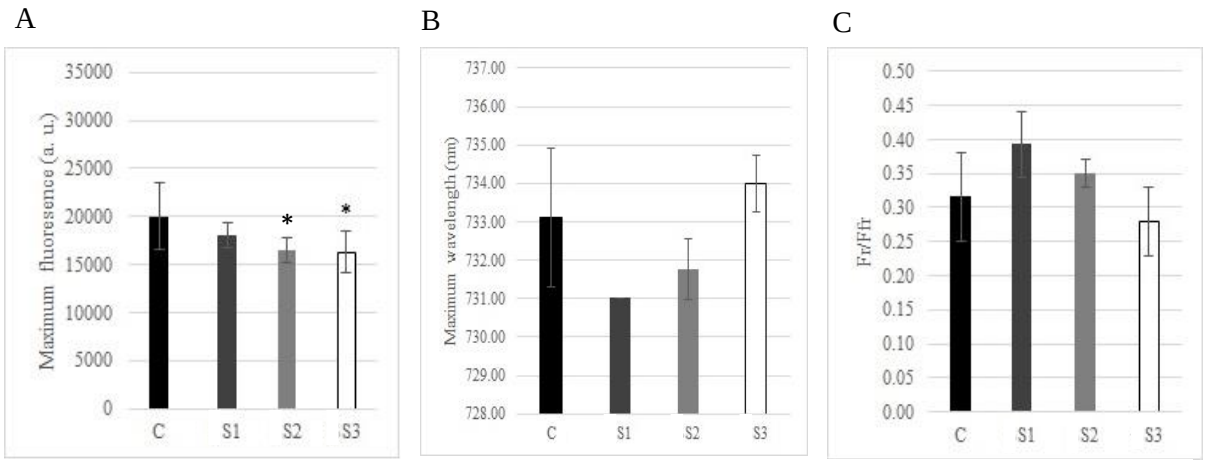

Fig. 5. Chlorophyll fluorescence response of *Glycine max* leaves under drought. (A) Maximum fluorescence emitted by chlorophyll; (B) Wavelength at which maximum fluorescence is emitted; (C) Ratio between fluorescence in the red region and in the far-red region. Fr, fluorescence in the red region; Ffr, fluorescence in the far-red region. C, control; S1, moderate stress; S2, severe stress; S3, extreme stress. Average values ± standard deviation is shown, n = 14 for C; n = 3, 9 and 8 for stress treatment, statistically significant differences from the controls are denoted by *.

4.4 Photosynthetic machinery status in *Glycine max* under drought

The PSII quantum yield (Fv/Fm) remains unchanged in stress treatments (Fig. 6A). Both ETR_{max} and α show a decrease in all stress levels, when comparing to the control group (Figs 6B and 6C). This response is even more pronounced in S3.

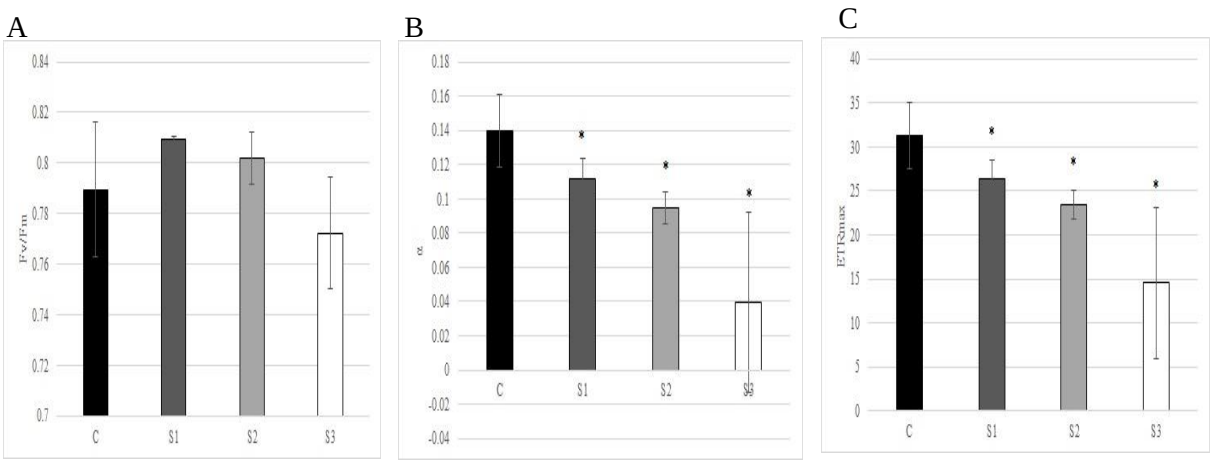

Fig. 6. *Glycine max* photosynthetic apparatus behaviour under drought. (A) Fv/Fm, maximum quantum yield of primary PSII photochemistry; (B) α, light harvesting efficiency of photosynthesis; (C), Maximum ETR, maximum electron transport rate. C, control; S1, moderate stress; S2, severe stress; S3, extreme stress. Average values ± standard deviation is shown, n = 5 for C; n = 3 for stress treatment, statistically significant differences from the controls are denoted by *.

In Fig. 7 the parameters related to energy transduction pathway (absorption, trapping, transport and dissipation) normalized per leaf cross-section (CS) are presented. S1 and S2 did not exhibit changes in dissipated energy, as well as in the electron transport flux, however, absorbed and trapped energy decreases in both. Noticeable changes are observed in S3, where absorbed, trapped and dissipated energy increase. At the contrary, electron transport flux diminishes. The number of active reaction centers per CS did not show any significant alteration under the tested conditions.

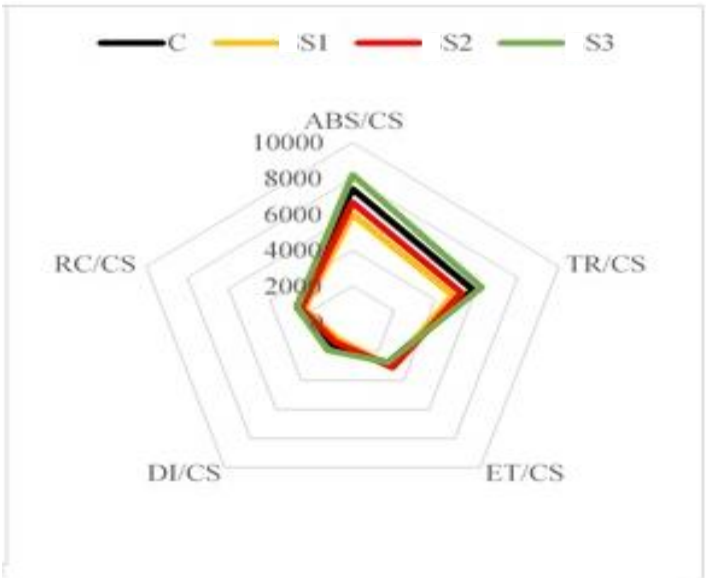

Fig. 7. Energy use and electrons behaviour in the ETC of *Glycine max* leaves under drought. ABS/CS, absorbed energy flux per cross section; TRo/CS, trapped energy flux per cross section; ETo/CS, electron transport flux per cross section; RC/CS, reduction energy flux per cross section; DIo/CS, energy dissipation as heat per cross section. C, control; S1, moderate stress; S2, severe stress; S3, extreme stress. N = 5 for C and n = 3 for stress treatment.

4.5 Pigment content in *Glycine max* leaves

Photosynthetic pigments contents were determined spectrophotometrically and results are shown in Fig. 8. Chlorophyll is expressed by leaf area. Chl *a* content did not change in leaves under stress (Fig. 8A). When analyzing both chlorophylls *a* and *b* through Chl *a/b* ratio, a significant decrease is observed in S1 and S2 when comparing it to control, but the value returns to control levels at S3 (Fig. 8B).

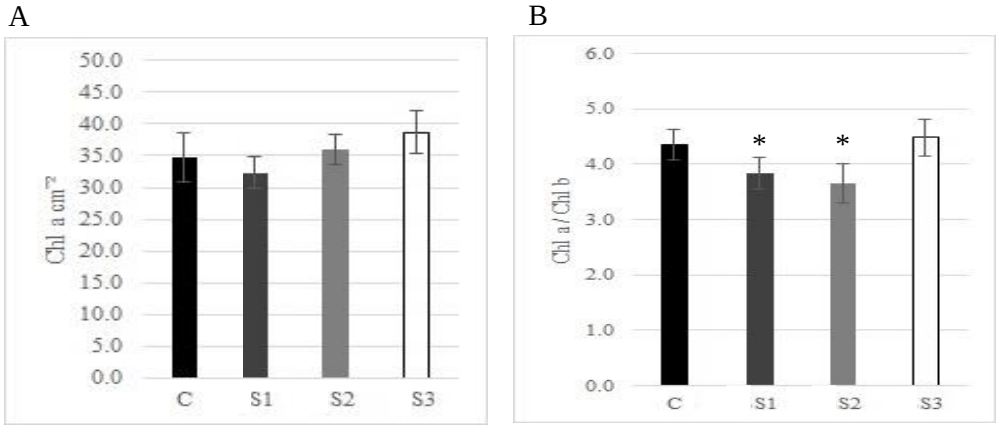

Fig. 8. Chlorophyll content in *Glycine max* leaves under drought. (A) Chlorophyll *a* expressed as area units; (B) Ratio between chlorophyll *a* and chlorophyll *b*. Chl, chlorophyll. C, control; S1, moderate stress; S2, severe stress; S3, extreme stress Average values ± standard deviation is shown, n = 16 for C; n = 10, 16 and 12 for stress treatment, statistically significant differences from the controls are denoted by *.

4.6. Lipid and fatty acid composition of *Glycine max* leaves

The relative amounts of the major lipid classes present in *Glycine max* leaves under different drought levels are shown in Fig. 9. After an increase under moderate stress, MGDG percentage show a decreasing trend, when comparing S2 and S3 with the control group. DGDG content also decreased as the severity of the stress increased and a similar trend was observed for phosphatidylethanolamine (PE). Phosphatidylcholine (PC) exhibited a transient decrease at S1, recovering to control levels at S2 and decreasing again at S3. Phosphatidylglycerol (PG) remained unchanged in all treatments, similarly to phosphatidylinositol (PI). However, the most important changes were in the neutral lipids fraction, in which TAG is included. Neutral lipids proportion increased very significantly with increasing water loss.

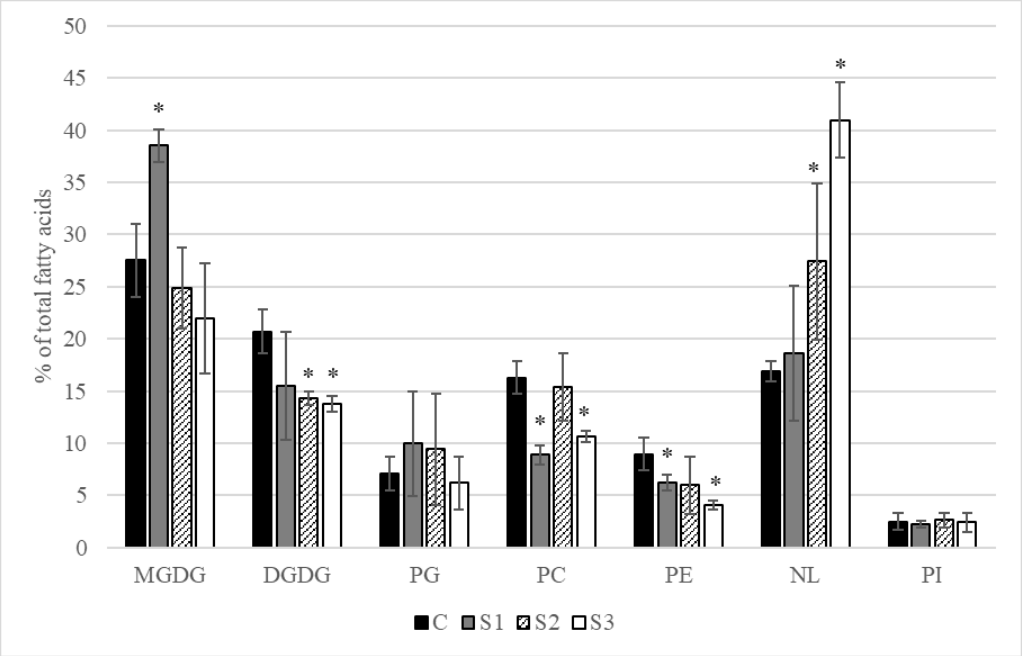

Fig. 9. **Effect of drought on the total fatty acid content in each lipid class of *Glycine max* leaves**. MGDG, monogalactosyldiacylglycerol; DGDG, digalactosyldiacylglycerol; PG, phosphatidylglycerol; PC, phosphatidylcholine; PE, phosphatidylethanolamine; NL, neutral lipids + free fatty acids; PI, phosphatidylinositol; C, control; S1, moderate stress; S2, severe stress; S3, extreme stress. Average values ± standard deviation is shown, n = 3, statistically significant differences from the controls are denoted by *.

In fact, in severe and extreme conditions, the ratio membrane lipids: neutral lipids decreased expressively (Fig. 10).

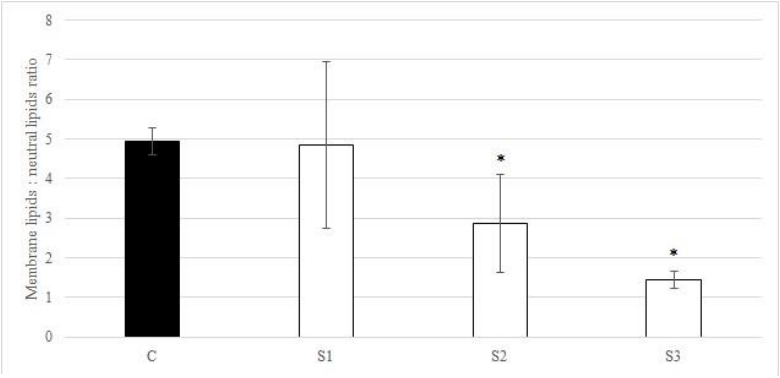

Fig. 10. Membrane versus neutral lipid proportions in *Glycine max* leaves under drought. Membrane lipids content regarding neutral lipid content. C, control; S1, moderate stress; S2, severe stress; S3, extreme stress. Average values ± standard deviation is shown, n = 3, statistically significant differences from the controls are denoted by *.

In Table 1 the distribution of the six fatty acids present in *Glycine max* leaves is represented: palmitic acid (C16:0), *trans*-hexadecanoic acid (C16:1t), stearic acid (C18:0), oleic acid (C18:1), linoleic acid (C18:2) and linolenic acid (C18:3). The percentage of C18:3 decreased in MGDG and the same tendency was seen in DGDG, while it increased in PC and neutral lipids. In contrast, the relative amounts of C18:2 decreased strongly in PC, PE and neutral lipids and decreased slightly in DGDG and MGDG, respectively. C18:1 content increased significantly in neutral lipids and did not vary in DGDG.

Table 1. Fatty acid composition of the major lipid classes from leaves of *Glycine max* plants under drought. MGDG, monogalactosyldiacylglycerol; DGDG, digalactosyldiacylglycerol; PG, phosphatidylglycerol; PC, phosphatidylcholine; PE, phosphatidylethanolamine; NL, neutral lipids + free fatty acids; PI, phosphatidylinositol; C, control; S1, moderate stress; S2, severe stress; S3, extreme stress. C16:0, palmitic acid; C16:1, *trans*-hexadecanoic acid; C18:0, stearic acid; C18:1, oleic acid; C18:2, linoleic acid; C18:3, linolenic acid. Average values are shown, n = 3, statistically significant differences from the controls are denoted in bold.

		C16:0	C16:1*t*	C18:0	C18:1	C18:2	C18:3
MGDG	C	4.4	0	4.4	0.6	3.6	86.9
	S1	2.3	0.1	**1.3**	1.1	**2**	**93.2**
	S2	3.8	0	5.3	0.9	**2.8**	87.1
	S3	4.6	0	8.3	1.2	**2.9**	83.1
DGDG	C	8.9	0.3	6.9	0.8	2.4	80.7
	S1	15.3	0.1	5.4	0.5	**1.8**	76.9
	S2	11.5	0.2	10.7	1.3	2.5	73.7
	S3	11.6	3.6	11.2	1.1	2.3	70.1
PG	C	38.5	17	18.4	8.1	6.5	11.6
	S1	31.9	21.2	13.5	6.4	12.1	14.9
	S2	34.4	10.6	21.9	**3.5**	**15.2**	14.4
	S3	37.1	18.1	20.3	6	7.8	10.6
PC	C	22.8	0	13.6	2.5	41.3	19.8
	S1	28	0	15.7	5.4	**24.8**	26.1
	S2	19.9	0	15	2	**23.5**	**39.6**
	S3	24.1	0	17	3.9	**25.5**	**29.5**

		C16:0	C16:1*t*	C18:0	C18:1	C18:2	C18:3
PI	C	37.6	0	37	4.4	14	6.9
	S1	39.9	0	24.9	3	16.1	16.1
	S2	37.2	0.6	36.5	4.5	10.9	10.3
	S3	41	0	45.1	1.9	**5.4**	6.6
NL	C	24	4.1	26.8	33.3	7.3	4.5
	S1	**12**	4.1	13.7	48	11.4	**10.7**
	S2	**13.7**	3.8	16.3	45.1	11.7	9.4
	S3	**14.6**	1.4	**14**	**45.6**	**12.1**	**12.4**
PE	C	28.2	0	18.4	2	39.3	12.2
	S1	28.9	0.4	10.7	2.6	36.8	20.6
	S2	27.8	0	32.9	4.8	**21.5**	13
	S3	31.1	0	32.7	1.3	**22.6**	12.4

The double bond index remained unchanged in MGDG, DGDG, PG, PC, PI and PE, while it increased in neutral lipids (Fig. 11).

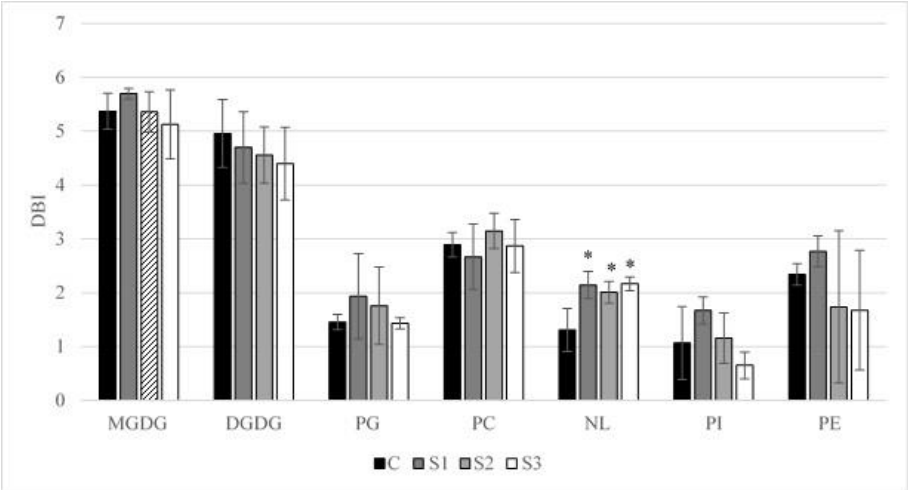

Fig. 11. Double bond index of the major lipid classes in *Glycine max* leaves under drought. DBI calculated as follows: 2 x (1 x % monodienoic acids) + (2 x % dienoic acids) + (3 x % trienoic acids) / 100. MGDG, monogalactosyldiacylglycerol; DGDG, digalactosyldiacylglycerol; PG, phosphatidylglycerol; PC, phosphatidylcholine; PE, phosphatidylethanolamine; NL, neutral lipids + free fatty acids; PI, phosphatidylinositol; C, control; S1, moderate stress; S2, severe stress; S3, extreme stress. Average values ± standard deviation is shown, n = 3, statistically significant differences from the controls are denoted by *.

The content of lipid peroxidation products, expressed as MDA equivalents increased strongly in S1 and S2 leaves but decreases in S3, although remaining higher than in the control (Fig. 12).

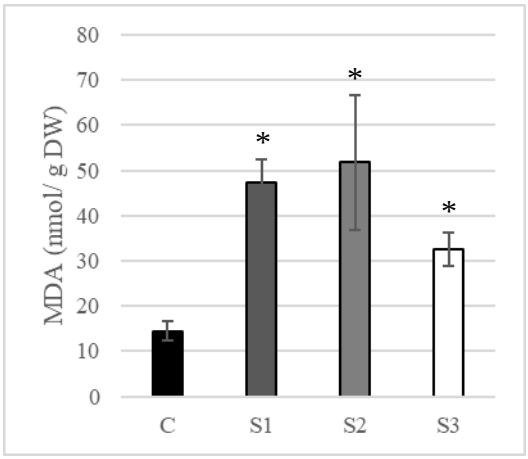

Fig. 12. MDA content in *Glycine max* leaves under drought expressed as g of dry weight. MDA, malondialdehyde. C, control; S1, moderate stress; S2, severe stress; S3, extreme stress. Average values ± standard deviation is shown, n = 3, statistically significant differences from the controls are denoted by *

4.7 Identification and Characterization of Phospholipase A Genes in *Glycine max*

We have identified 50 PLA genes in *Glycine max* genome encoding 55 proteins due to alternative splicing. Domain and motif analysis allowed PLA superfamily classification in four families: PLA1, PA-preferring PLA1, pPLA and sPLA2, with, respectively, 23, 1, 21 and 5 genes (Supplementary data 4). Moreover, families were divided into groups as follows: PLA1 was divided in groups I, II and III, with 17, 5 and 1 members, respectively and pPLA was divided in groups I, II and II with 2, 11 and 8 members, respectively. sPLA2 was represented by 5 genes and no groups were found (Supplementary Data 4).

4.8 Gene structure

The 50 PLA genes were mapped in *Glycine max* chromosomes. These genes were unevenly distributed among 17 out of the 20 chromosomes that constitute soybean genome. No PLA genes were found on chromosomes 4, 12 and 16. Chromosome 7 contained a higher number of PLA genes (8) than the other chromosomes (Fig. 13).

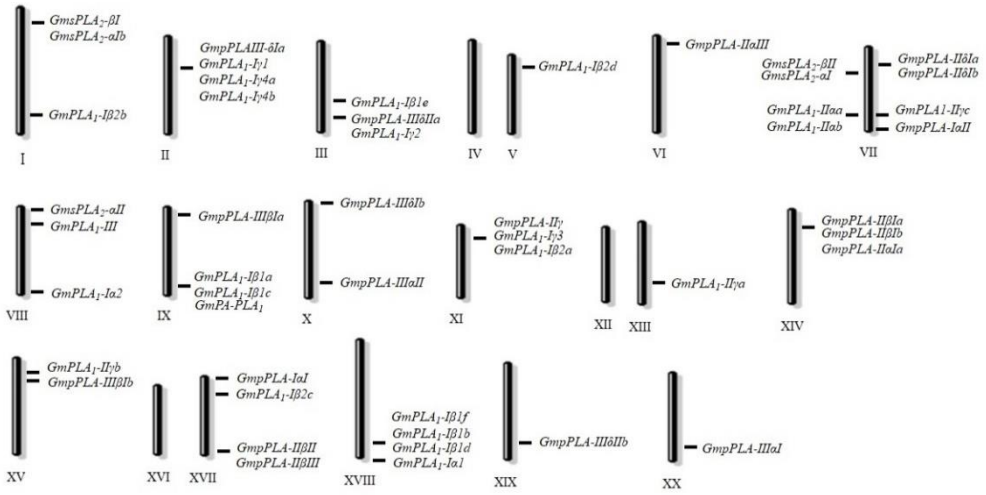

Fig. 13. Chromosomal localization of PLA genes on *Glycine max* genome. Genes from different PLA classes have been mapped by their position on 17 out of the 20 *Glycine max* total chromosomes. Respective chromosome roman numeration is mentioned at the bottom. In each chromosome, gene proposed nomenclature (Supplementary data 4) is shown.

In order to study gene structure, intron-exon analyses were performed. Thirteen PLA1-I and one PLA1-III genes are intronless, whereas PLA1-II genes all present 1 intron. pPLA-I genes present a structure with 17-18 introns, while pPLA-II has 5-6 introns and pPLA-III introns number range from 1 to 3. PA-preferring PLA1 is the class with highest number of introns (19). sPLA2s genes present 2-3 introns (Supplementary data 4).

4.9 Protein Structure, Subcellular Location and Domain Analysis

Molecular weight and isoelectric point (pI) were predicted for *Glycine max* PLA proteins. pPLA-I was the group with highest predicted molecular weight, ranging from 120 to 140 kDa. The majority (81%) of PLAs exhibited a molecular weight between 41 and 60 kDa. sPLA2s were the family with lowest molecular weight predicted, from 14 to 17 kDa (Supplementary Data 4).

Glycine max PLAs had a theoretical pI between 5.72 and 9.48. pPLA-I was the subfamily which pI is globally lower, around 5.83, indicating that pPLA-I proteins are acidic, while in other families this parameter was very uneven (Supplementary Data 4).

All pPLA-I and PLA1-III proteins were predicted to be located in the chloroplast. The remaining pPLAs and PLA1s were heterogeneously distributed, being located in cytosol (8), endoplasmic reticulum (ER) (3), nucleus (1), mitochondria (3), peroxisome (1) and in the extracellular matrix (4). Nevertheless, chloroplast was the main organelle in which PLAs are located (62%) (Supplementary data 4).

Multiple sequence alignment analysis of PLA families confirmed the presence of highly conserved catalytic motifs. All PLA1 members had a highly conserved GxSxG motif that included de Ser residue from the catalytic centre, while all group I and II pPLA members were found to harbour the characteristic esterase box GTSTG (except in group III where the Ser residue is replaced by a Gly residue) and the anion binding DGGGxRG motif, as well as the further specific motifs such as SAAPTY and DGGxxANN, containing the D residue (Asp), as part of the catalytic dyad. sPLA2 contained a PA2c domain denoted by the YGKYCGxxxxGC motif and the catalytic site LDACCxxHDxCV (Fig. 14). Other motifs were found: members of the pPLA-I group presented leucin-rich repeats (LRR8) and an armadillo motif, whilst all pPLA subfamilies shared the patatin domain, which was the only domain found in both pPLA- II and pPLA-III groups. PLA1s proteins shared a lipase 3 domain. No domains were found for the sPLA2 family (Supplementary data 4).

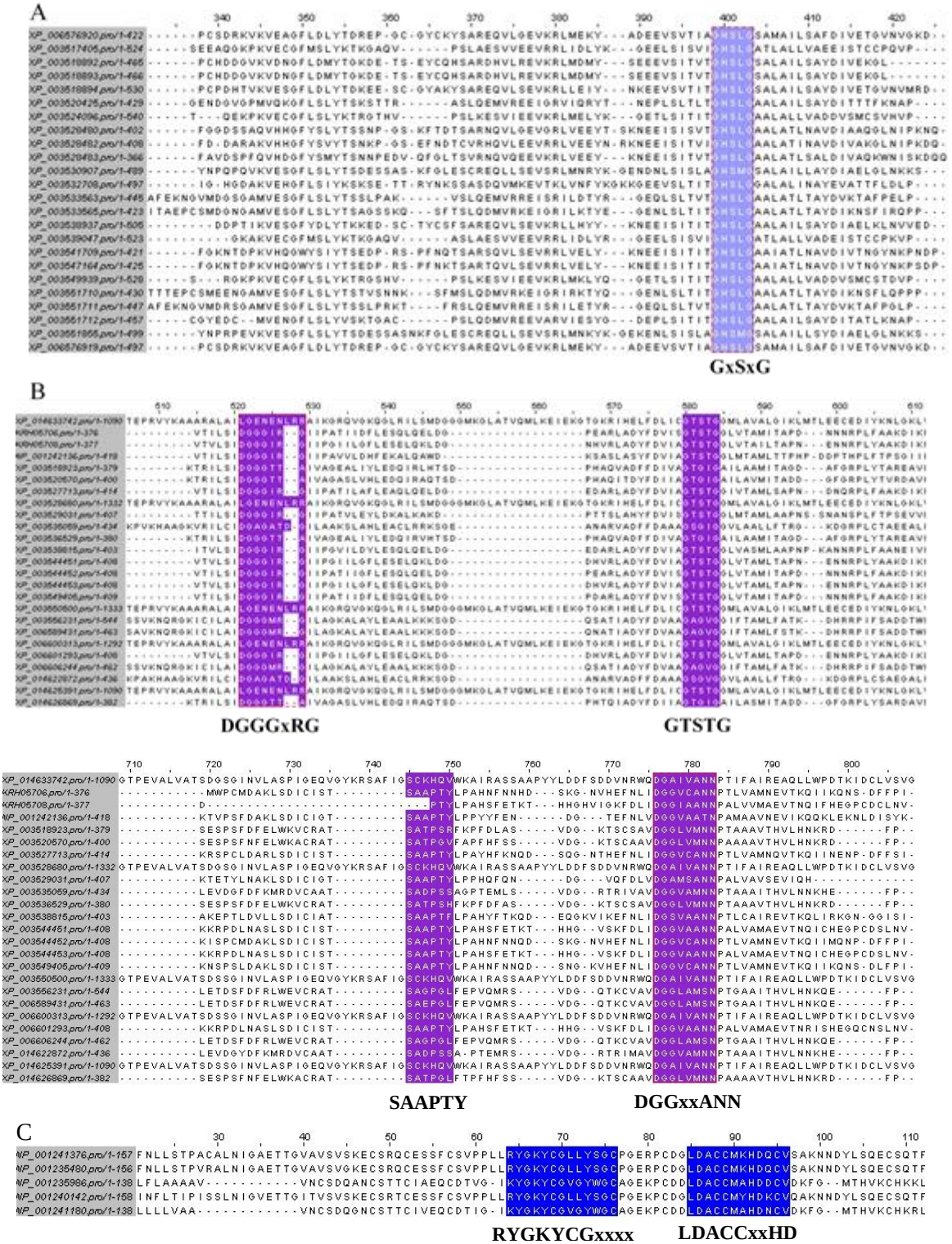

Fig. 14. Multiple sequence alignment of (A) PLA1 (B) pPLA and (C) sPLA showing conserved motifs. Protein sequences were aligned for each PLA family, separately applying Clustal W tool of MegAlign – DNASTAR. Conserved sequences are coloured.

4.10 Phylogenetic analysis

A phylogenetic analysis of the 55 soybean PLA proteins was carried out and the consensus phylogeny obtained is shown in Supplementary data 2. Four families, pPLA, PLA1, PA-preferring PLA1 and sPLA2 were identified and the first two were still divided in different, well differentiated clades, representing subgroups I, II and III. Exception for sPLA2 where no groups were defined.

For each PLA family, pPLA, PLA1, PA-preferring PLA1 and sPLA2, a new phylogenetic analysis was done including both soybean and *Arabidopsis* amino acid sequences (Fig. 15). All the three PLA classes were divided into different clades representing subgroups. Members of the same subgroup in a PLA class for both *Arabidopsis* and soybean seemed to have high degree of evolutionary relatedness and some divergence from the members of the other subgroups (Supplementary data 2). This pattern suggests the common ancestry of PLAs in the two diverse plant species, and was used for the classification and nomenclature of the genes in soybean as previously accorded (Scherer *et al*., 2010) (Supplementary data 4).

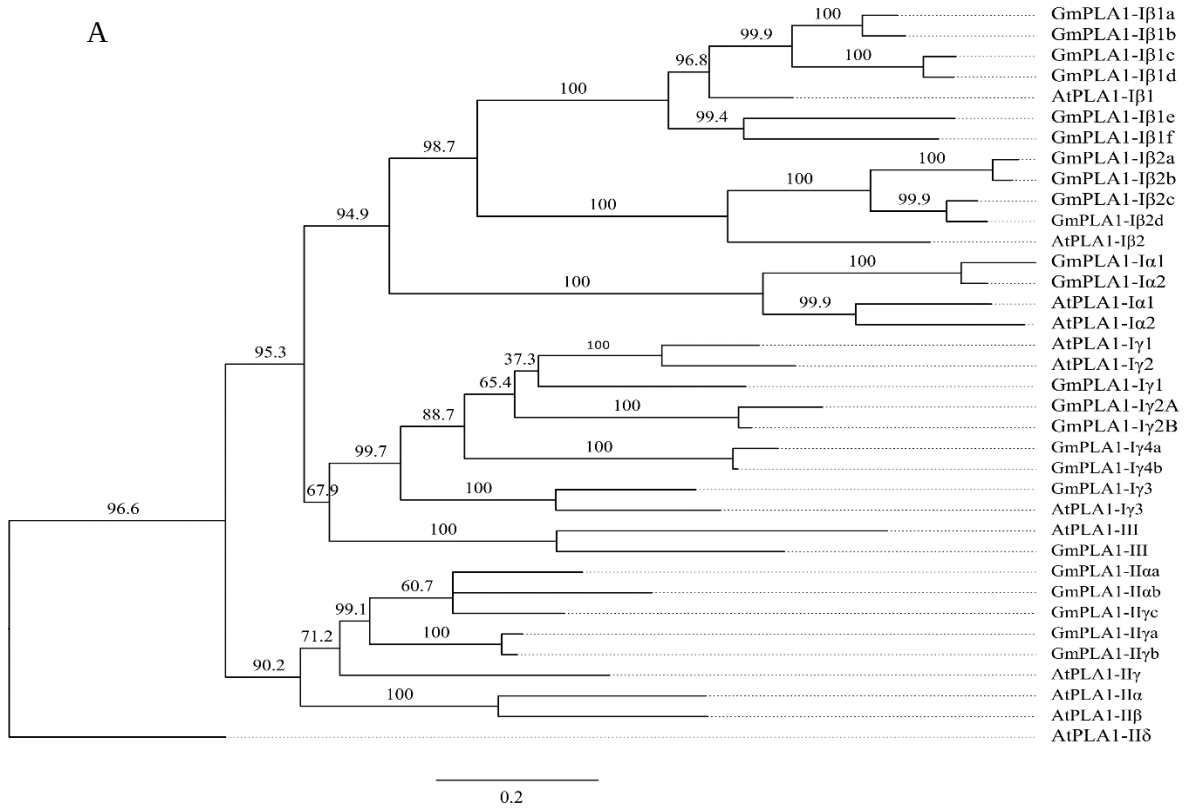

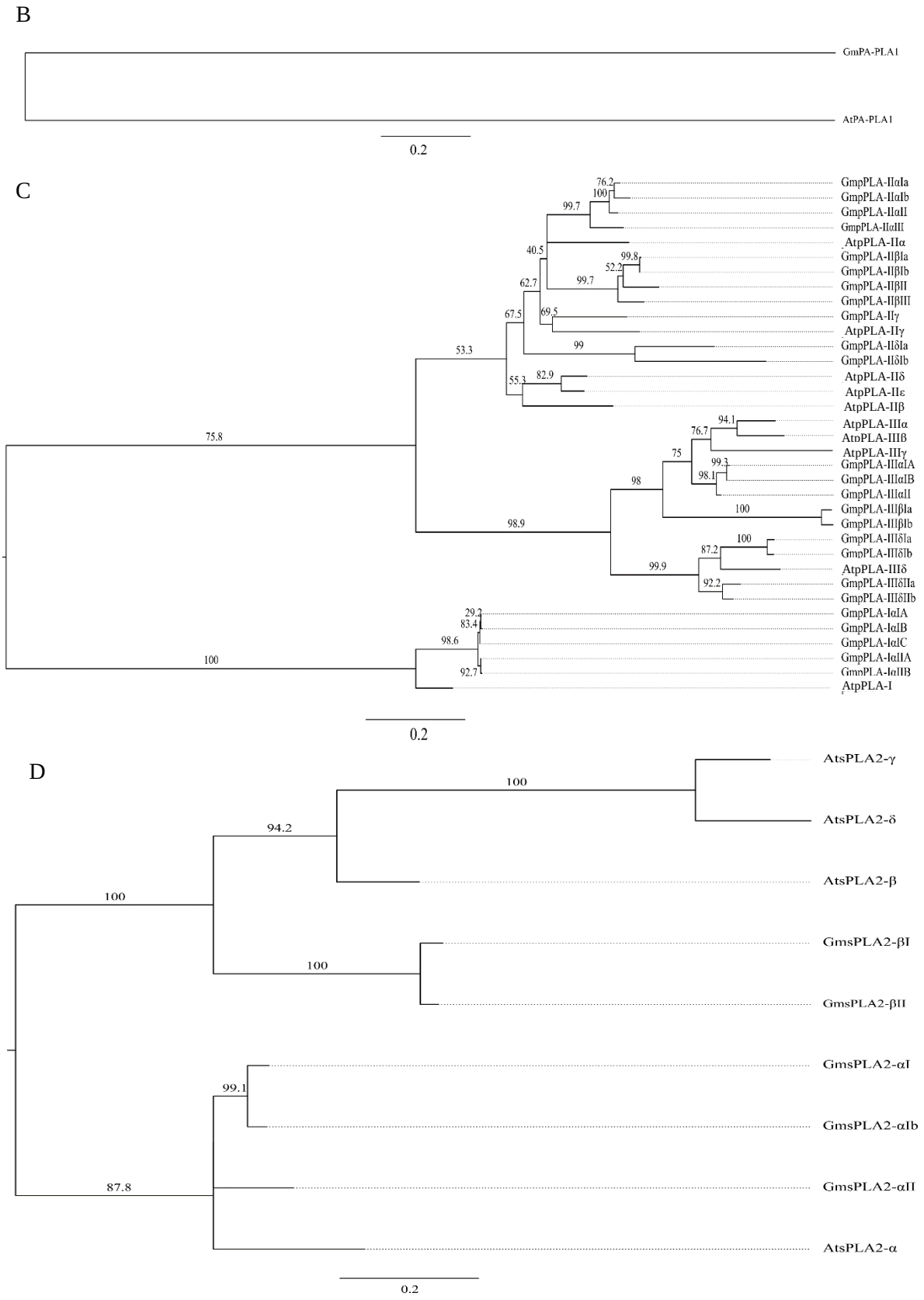

Fig. 15. Phylogenetic relationship between *Glycine max* and *Arabidopsis thaliana* PLA superfamily. A rooted BioNJ based tree was generated from protein sequences of *Glycine max* and *Arabidopsis thaliana* PLAs, separately by families (A)PLA1; (B) PA-preferring PLA1; (C) pPLA and (D) $sPLA_2$. Multiple sequence alignment was done using Clustal W and tree was generated using MegAlign Bootstrap value, out of 1000 replicates is indicated at each node. Scale bar represents 2.0 amino acid substitutions per 100 residues.

4.7. Gene expression

To investigate expression of genes coding for phospholipases A and other lipid metabolism related enzymes, a qPCR analysis of the following genes was performed: PLA1-I (*GmPLA1-Iβ1c*), PLA1-II (*GmPLA1-IIγa*), PLA1-III (*GmPLA1-III*), pPLA-I (*GmpPLA-IαII*), pPLA-II (*GmpPLA-IIαIa*), pPLA-III (*GmpPLA-IIIαII*), sPLA2 gene (*GmsPLA2-αI*), DGAT (*GmDGAT1C*), PDAT (*GmPDAT1E*) (Li *et al*., 2013) and FAD3 (*GmFAD3C*) (Torres-Franklin *et al*., 2009), (Supplementary data 1).

pPLA-III expression levels seemed to be directly correlated to increasing drought severity, being strongly up-regulated when comparing to the control group. PLA1-III coding gene was down-regulated in moderate and severe drought but increased its expression in extreme water deficit (Fig. 16). pPLA-II showed a similar response to PLA1-III, being down-regulated in S1 and S2 but up-regulated in S3 (Fig. 16). PLA1-II was significantly up-regulated under moderate stress, S1, when comparing to the control group but its expression decreased progressively until the extreme stress stage. Yet, at all stages of drought, it was up-regulated. pPLA-I was up-regulated, slightly increasing its expression at all stages of drought (Fig. 16). On the contrary, sPLA genes were shown to be down-regulated in all drought levels. The DGAT gene was up-regulated at all stages of water stress and PDAT was down-regulated, but both vary very slightly from the control (Fig. 16).

Under drought stress, FAD3 was the gene that showed the greatest significant differences, being strongly down-regulated especially in S3 (Fig. 16).

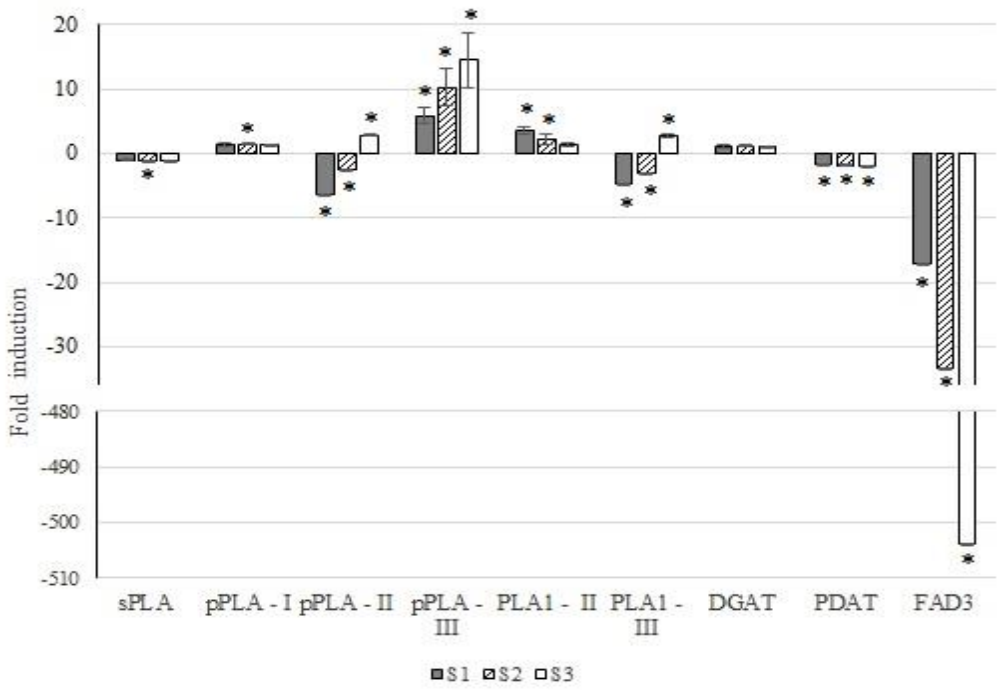

Fig. 16. Expression of PLA and other genes encoding lipid metabolism enzymes in *Glycine max* leaves under drought. Relative expression, comparing to control is shown for *GmsPLA2-αI, GmpPLA-IαII; GmpPLA-IIαIa; GmpPLA-IIIαII; GmPLA1-IIγa; GmPLA1-III; GmDGAT1C, GmPDAT1E* and *GmFAD3C*. S1, moderate stress; S2, severe stress; S3, extreme stress Average values ± standard deviation is shown, n = 3, statistically significant differences from the controls are denoted by *.

No consistent results were obtained for PLA1-I due to extremely low transcript abundance (not shown). In control conditions, the PLA that showed more expression was sPLA, with a Ct value of 22.9 ± 0, followed by pPLA-III with a Ct of 25.8 ± 0.7 and PLA1-II having an average Ct of 27.2 ± 0.3. The other PLA studied genes have Ct values around 30. Since PLA are lipolytic enzymes, it is understandable that in control conditions, they are expressed at very low levels (Supplementary data 1).

5. Discussion

Previous studies have shown that plants lipid metabolism is highly affected by water stress (Gigon *et al*., 2004; Pham-Thi *et al*., 1990). In the present study, we aimed to access soybean fatty acid modulation in drought stress conditions and to study the involvement of phospholipase A genes in FA modifications.

5.1. *Phenotypic response to drought*

When water stress is imposed, stomata closure is one of the first response mechanisms in order to lower transpiration rate (Manavalan *et al*., 2009), having as consequence an inevitable reduction of the leaf thermal regulation capacity and a correspondent increase in leaf temperature. This last response can be easily accessed by thermal imaging (Martynenko *et al*., 2016). In fact, in soybean leaves under stress, thermal imaging data revealed that leaf temperature increased quickly and remained permanent in the 3rd day, which corroborates the previously described by Martynenko and co-workers (2016), where after the 3rd day, plants surpassed the "Iwanov" effect, which is a rapid initial stomata opening before the long-term closure in conditions of water deficit that cause a slight decrease of temperature and only then a permanent increase in temperature was observed.

5.2. Photosynthesis is impaired under drought

Damages in photosynthetic apparatus can be analysed through chlorophyll fluorescence evaluation methods such as LIF and PAM that allow *in vivo* monitorization, in a non-invasive manner (Baker *et al*., 2004).

For the LIF technique it has been shown that two chlorophyll emission fluorescence peaks are detected: a local maximum in the red region (685-690 nm) and an absolute maximum at the far-red region (730-735nm) (Hák *et al*., 1990). The intensity, shape and wavelength of these peaks change when alterations in the photosynthetic machinery occur (Gameiro *et al*., 2016). In soybean under drought stress, it was not possible to observe an effective peak in the red region. Nevertheless, alterations occurred in the far-red peak, with a decrease in the maximum fluorescence. Changes in fluorescence can be related to chlorophyll content (Buschmann, 2007), however, since no changes in Chl *a* content were in general observed, other causes previously reported cannot be excluded, such as leaf structure and optical properties. In fact, Gausman *et al.* (1973) evidenced that soybean leaves have a low absorption coefficient and a relatively high reflectance, thus, when subjected to water stress, these features tend to stand out.

The low fluorescence in leaves under stress might be due to damages in the PSI, since this structure contains the so-called "far red chlorophylls", absorbing at wavelengths beyond 700 nm (Pettai *et al*., 2005) and if impaired, absorption and emission could be diminished. LIF technology has already revealed that Fr/Ffr ratio is associated with chlorophyll concentration, in many species, under drought stress, showing an inverse curvilinear relationship (Caires *et al.*, 2012, Gameiro *et al*., 2016). In fact, Fr/Ffr ratio is chlorophyll dependent and decreases with increasing chlorophyll content (Gitelson *et al*., 1998). In soybean, chlorophyll concentration revealed an increasing trend that is inverse to the trend observed in Fr/Ffr ratio. The fact that chlorophyll concentration did not significantly vary may be due to the shrinking of the leaves caused by water loss, thus turning chlorophyll concentration higher, similarly to what occurred in *Arabidopsis thaliana* (Gameiro *et al*., 2016). Also, Chl *a/b* ratio decreases very slightly in S1 and S2, indicating that the size of the PSII antennae is not much affected. Moreover, Chl *a/b* ratio is a common stress indicator, with low values indicative of photochemical stress at the PSII antennae (Duarte *et al*., 2015). This is in contrast to what has been observed earlier in other species, namely in two lines of *Okra* in which chlorophyll *b* content increased whereas chlorophyll *a* remained unaffected resulting in a significant pronounced reduction in Chl *a/b* ratio (Jaleel *et al*., 2009).

As mentioned above, PAM is commonly used to infer about photosynthetic apparatus condition. PAM parameters allow the monitoring of the electron transport chain (ETC). The maximum quantum yield of primary PSII photochemistry (Fv/Fm) is widely studied in *Glycine max*. In the present work, it did not show significant changes. In fact, previous studies in other soybean cultivars, Tanbakuro and Tamanishiki, subjected to drought, revealed that Fv/Fm parameter remained unchanged when compared to the control group (Ohashi *et al*., 2004). Cultivar CD202 also did not change, except in the rapid drought treatment (Bertolli *et al*., 2012). These non-occurred changes in most treatments, show that leaf photochemistry was rather resistant to water stress.

After theoretical being excited in PSII, electron flow through ETC. Our results revealed that with increasing drought treatment, it is possible to note a decrease in the maximum electron transport rate through the ETC. Prior investigations, confirmed in this work revealed that ETR decrease is more sensitive than Fv/Fm decrease, ascertain that the PSII is quite resistant, since potential photochemical efficiency is not readily affected by water deficiency (Souza *et al*., 2013). Like ETR, parameter α is also extracted from the light curve and is a measure of the light harvesting efficiency of photosynthesis. In the present study, it is possible to see that photosynthetic efficiency follows the trend of the maximum ETR, meaning that the main cause for its reduction that happens in S1 and S2 might be a less effective ETC. A possible explanation might be because lower electron transport rate negatively affects photophosphorylation hence decreasing ATP synthesis and $NADP^+$ reduction in the light dependent phase of photosynthesis and therefore, these compounds cannot be used in the Calvin cycle, impairing the whole process (Lisar *et al*., 2012).

The absorbed energy flux per cross section increased with increasing water loss. Under stress conditions it is often observed an increase in the light absorption in order to overcome possible impairments at the ETC (Duarte *et al*., 2016). Alongside a proportional increase in trapped energy flux was also observed, indicating a normal function of the PSII antennae, also in accordance to what was previously mentioned regarding Chl *a/b* ratio. Nevertheless, the impairment of the ETC due to low quinone redox turnover rate, generates high amounts of reducing power at the PSII donor side, therefore, in order to avoid PSII damage by D1 protein destruction due to highly negative redox potential, the electronic energy has to be dissipated (Duarte *et al*., 2016). The same behaviour was previously observed in two cultivars of *Vitis amurensis* (Wang *et al*., 2012b). ETC is found in the membranes, thus, changes in membrane lipid composition influence ETC function.

5.3. Lipid modulation under drought

In plants, drought stress is first perceived by membranes, which respond in order to maintain membrane homeostasis and through the release of messengers that trigger signaling cascades (Gasulla *et al*., 2013). In soybean under water deficit, all membrane lipids besides PI, exhibit a decreasing trend, particularly in S3 treatment. Thus, conformational changes in membranes and alterations in cell structure have likely occurred in response to drought, similar to previously described in *Arabidopsis thaliana* (Gigon *et al*., 2004). Prior studies in *Arabidopsis thaliana* (Gigon *et al*., 2004), cotton (Pham-Thi *et al*., 1985) and coconut tree (Repellin *et al*., 1997) showed that from all of the lipid classes affected by water stress MGDG was the most sensitive to degradation, and the same was verified here in *Glycine max*. This decrease in MGDG fatty acids may be related to either minor biosynthesis rate or fast lipolytic turnover. DGDG content also decreased, which is contrary to the previously described for *Arabidopsis thaliana*, but in accordance with results obtained for drought-sensitive *Vigna unguiculata*, cvs 1183 and IT83D (Gigon *et al.*, 2004; Torres-Franklin *et al*., 2007; Pham-Thi, *et al*., 1990). Neutral lipids comprise free fatty acids (FFA), DAG and TAG. Therefore, the increase observed in this group might be due to either increase of FFA and/or TAG or both. However, since FFA act as membrane detergents, these molecules are never found in high concentrations, including under water deficit (Matos *et al*., 2008). Since previous data on *Glycine max* revealed that TAG increases under drought conditions (Martin *et al*., 1986), it is

likely that the same have occurred in the present work. TAG is not a common lipid in leaves, since it is a storage lipid, hence being mostly found in seeds. However, environmental stresses leading to precocious leaf senescence can also induce TAG accumulation (Matos and Pham-Thi, 2009; Kaup *et al*., 2002). Thus, TAG may be stored in soybean leaves under drought stress through recycling of FA resulting from galactolipid degradation by the action of plastidial PLA. FFA, after entering the Acyl-CoA pool, are used to acylate DAG at sn-3 position, by the action of DGAT, to generate TAG. Another enzyme involved in TAG synthesis is PDAT which transfers an acyl group from PC to the *sn*-3 position of DAG. The lyso-PC molecule formed is then converted back in PC by LPCAT (Lysophosphatidylcholine acyltransferase) through a process designated Lands cycle (Chapman *et al*., 2012).

C18:3 was found as the most abundant fatty acid in all lipid classes analyzed, especially in both galactolipids MGDG and DGDG. Martin and co-workers (1986) observed that C18:3 decreased in these lipids in an advanced stress status. In fact, our results show a decreasing trend on this fatty acid in both galactolipids. This can result from direct reaction with reactive oxygen species, which accumulate in water deficit conditions, as well as an increase in the lipolytic activity of PLAs (Gameiro *et al*., 2016). In contrast, in PC, there was a rise in C18:3, which was already observed by Martin *et al*. (1986). DGDG, PC, and PI reveal an increasing trend in their C16:0 and C18:0 content, while neutral lipids significantly decrease the content of the same fatty acids, which is in agreement with previous data (Martin *et al*., 1986).

DBI is a parameter that represents the fatty acid desaturation level and is related to membrane fluidity. However, in the six studied lipids, it remained unaltered, similarly to what was previously observed in Arabidopsis for MGDG, DGDG, PG and PC (Gigon *et al*., 2004). Neutral lipids increased their desaturation in S1-S3, that could be possibly due to accumulation of C18:3.

Lipid peroxidation resulting products, namely, MDA, is showed to be accumulated under stress conditions. This result is in agreement to what has been observed in tomato leaves in moderate and severe stress as well as in rice (Yuan *et al*., 2016, Farooq *et al*., 2009). This peroxidation in the membranes is the result of free radical induced damage at the cellular level (Nouairi *et al*., 2008).

In *Glycine max*, the changes observed in lipid content and composition influence photosynthesis efficiency. The decrease in galactolipids, the increase in saturated fatty acids and the decrease in C18:3 decrease membrane fluidity (Leekumjorn *et al*., 2009), resulting in impairment of light harvesting efficiency of photosynthesis and in ETR_{max}.

5.4. *Glycine max* phospholipase A superfamily

A preliminary characterization of the PLA superfamily started in 2013 (Machado *et al*., 2013; Machado *et al*., 2013), however, updates in *Glycine max* genome databases were performed in the meantime. In the present work, we were able to identify 50 PLA genes in *Glycine max* genome encoding 55 proteins, which indicates the existence of alternative splicing. In fact, several isoforms were found for both pPLA-I, pPLA-III and PLA1-I genes. Phylogenetic analysis showed that, similarly to *Arabidopsis thaliana* (Ryu, 2004) and *Oryza sativa* (Singh *et al*., 2012), *Glycine max* presents four well defined families: PLA1, PA-preferring PLA1, pPLA and sPLA2. PLA1 and pPLA families were further divided in three subgroups (I, II and II), Based on Ryu (2004) and with the re-annotated pPLA names (Scherer *et al*., 2010), a nomenclature was suggested for PLA genes in *Glycine max*. To support phylogenetic data division in families, domain analysis by Pfam placed the lipase 3 domain in PLA1 members and the patatin motif in pPLAs (Supplementary data 4), similarly to what was earlier reported in *Arabidopsis thaliana* and *Oryza sativa* (Ryu, 2004; Singh *et al*., 2012). Previous studies in *Glycine max* have already observed the existence of the PA2c domain in sPLA as well as 12 conserved Cys residues (Mariani *et al*., 2012). Moreover, the referred lipase 3 motif comprises a common GxSxG sequence, containing the catalytic Ser residue of the active site (Richmond *et al*., 2011) in which the second residue is always a

histidine and the fourth can either be a Leu or a Met residue in *Glycine max*. Also, the patatin domain that includes the catalytic center GTSTG (Scherer *et al*., 2010) was also found in soybean. Soybean PLAs were mainly located in chloroplast (62%). This is in accordance to the previously described in rice, where 42% of PLAs are located in chloroplast (Singh *et al*., 2012).

Gene structure analysis revealed that from the 23 PLA1 genes mostly are intronless, exception made for 5 PLA1-I group with 2 introns and 5 PLA1-II group with 1 intron, (Supplementary data 1), which is specific for *Glycine max*, since in most species, namely, *Arabidopsis thaliana*, PLA1 genes are intronless (Singh *et al*., 2012; Matos and Pham-Thi, 2009). Morevoer, in general, intron-exon analysis in *Glycine max* differs from that in *Arabidopsis thaliana* and *Oryza sativa*, both in number and majority/minority distribution in families. Three sPLA genes have 3 introns while 2 have 2 introns, like previously seen in *Glycine max* (Mariani *et al*., 2012). The fact that some PLAs from the same family share the same number of introns/exons might be indicative of divergence events and duplication. Chromosomal mapping of *Glycine max* PLA genes showed their uneven distribution in 17 of the total 20 chromosomes that constitute soybean genome. No PLA genes were found on chromosomes 4, 12 and 16.

5.5. Gene expression

PLAs are responsible for decreasing polar lipid content, affecting particularly the levels of MGDG. In the present work, it was analyzed one gene of each PLA family, chosen according to microarray publicly available data (Le *et al*., 2012). Hence, the genes that were up-regulated under drought with higher folds were selected. In *Glycine max*, the most expressed phospholipase is pPLA-III, whose gene was up-regulated in all drought stages and at S3 exhibited the most relative quantity. This result, confirmed previous microarray data, in which, it has a 6.29-fold change (Table 2), agrees as well with previous results in Arabidopsis, where up-regulation of pPLAIIIβ was observed (Matos *et al*., 2008). PLA1-II gene displayed the highest fold increase at S1 decreasing thereafter its expression until S3. PLA1-III gene showed a similar behavior to that of pPLA-II, being up-regulated only in S3, indicating its role in lipid degradation linked to senescence. pPLA-II gene remained down-regulated in S1 and S2, although increasing expression so that in S3 is already being up-regulated significantly. Up regulation of pPLA-II orthologous have been previously observed in *Vigna unguiculata* and *Arabidopsis thaliana* (Matos *et al.*, 2001; Matos *et al*., 2008). However, in both plants up-regulation under moderate stress was also observed, which could possible suggest a role in drought signaling, similarly to what has been proposed for this protein in the responses to other stresses (Scherer *et al*., 2010). It was not the case of the soybean isoform, however, given the high number of group II pPLA present in the soybean genome, it is possible that other paralogues fulfill this role. sPLA2 gene did not show variations and was down-regulated in S1-S3 plants, which differs from microarray results, that indicates a slight up-regulation of 1.39-fold change, only in one of the experiments. pPLA-I gene also did not show variations, although it was being up-regulated (Table 2). The expression of PLA1-I was undetectable in our samples likely indicating low transcript abundance. Supporting this idea is the fact that PLA1-I did not reveal the presence of EST, which may be indicative of very low expression under our experimental conditions or possibly be a pseudogene. In control conditions, pPLA-I, pPLA-II and PLA1-III studied genes were shown to be the least expressed, with Ct values of 29.6, 30.3 and 28.6, respectively.

Table 2. Microarray data crossed with relative cDNA concentration of PLA's family, DGAT, PDAT and FAD3 genes of *Glycine max* in S3. Microarray results from Le *et al*. (2012); V6, late vegetative stage; R2, full bloom reproductive stage; -, no microarray data available. Relative cDNA concentration is expressed as normalized relative quantities (NRQ). S1, moderate stress: S2, severe stress; S3, extreme stress.

Gene	Microarray data (Le *et al*., 2012)		S1 NRQ	S2 NRQ	S3 NRQ
	V6	R2			
GmsPLA2-αI	1.39	1.05	-1.09	-1.22	-1.26
GmpPLA-IαII	1.97	1.86	1.35	1.45	1.21
GmpPLA-IIαIa	1.21	3.62	-6.34	-2.51	2.80
GmpPLA-IIIαII	6.29	2.15	5.87	10.18	14.45
GmPLA1-Iβ1c	1.22	1.66	-	-	-
GmPLA1-IIγa	1.38	1.19	3.50	2.17	1.37
GmPLA1-III	-	-	-4.78	-3.19	2.64
GmDGAT1C	2.19	3.09	1.05	1.14	1.08
GmPDAT1E	2.29	2.11	-1.65	-1.87	-1.96
GmFAD3C	-	-	-17.20	-33.25	-503.69

Besides phospholipases, also DGAT, and PDAT and FAD3 were studied in order to understand the increase in NL, namely TAG content and its increase in C18:3 that occurs under drought stressed leaves. DGAT catalyze the irreversible conversion of diacylglycerol (DAG) into TAG through either recycling of FFA (C18:2 and C18:3), generated by PLA hydrolyzing activity on both phospho- and glycolipids or *de novo* fatty acid synthesis that enter the Acyl-CoA pool (Weselake *et al*., 2008), and PDAT uses PC as the acyl donor to transfer an acyl group to the *sn*-3 position of DAG to produce TAG (Liu *et al*., 2016). FAD3 is a desaturase located in the endoplasmic reticulum which converts C18:2 into C18:3 in extraplastidial lipids, including PC and PE. Results show that DGAT expression did not vary, while PDAT expression showed to be slightly down-regulated. These results are somewhat different from microarray, where DGAT and PDAT appeared to be slightly up-regulated. On the other hand, FAD3 strongly decreased its expression, similarly to what was previously verified in *Vigna unguiculata* (Torres-Franklin *et al*., 2009). Our results revealed that water deficit triggers an increase of C18:3 enriched PC and neutral lipids. This occurs in parallel with a decrease in the galactolipids content, normally very rich in C18:3. We hypothesize that fatty acids, mainly C18:3, are released from galactolipids from a plastidial PLA, enter the cytosolic Acyl-CoA pool and are incorporated in PC and in TAG, in a process possibly involving a cytosolic PLA and or PDAT. Since the increase of C18:3 in PC could have also resulted from increased activity of FAD3 we tested FAD3 gene expression. The fact that FAD3 gene expression is strongly repressed under water deficit favor our hypothesis of a transient accumulation of plastidial-derived C18:3 in PC, which is further channeled to TAG. Although in seeds DGAT catalyzes the last committed step in TAG biosynthesis and PDAT can also be involved in the biosynthesis of TAG from PC, it was expected that the expression of both genes would increase under our experimental conditions. Although we cannot exclude their increased contributions by stimulation of enzyme activity it is possible that TAG biosynthesis in leaves occurs by a different mechanism than the one operating in seeds, possibly with a contribution of PLAs (Fig. 17), (Kennedy *et al*., 1956; Lands, 1960).

We suggest, taking into account our gene expression results that the release of C18:3 from galactolipids might be mainly due to the hydrolysis activity of the studied *GmpPLA-IIIαII* gene that was showed to

be strongly up-regulated, but also through the studied *GmpPLA-IαII*, *GmPLA1-IIγα* and, in S3, *GmPLA1-III*, all located in the chloroplast. The release of C18:3 from PC (for posterior incorporation in TAG) could be due to the studied *GmpPLA-IIαIα*, in S3, rather than by PDAT, since it showed to be down-regulated (Fig. 17). However, the simultaneous contribution of the different pathways could not be excluded, since, although not up-regulated, both DGAT and PDAT genes are expressed at significant levels in soybean leaves under water deficit.

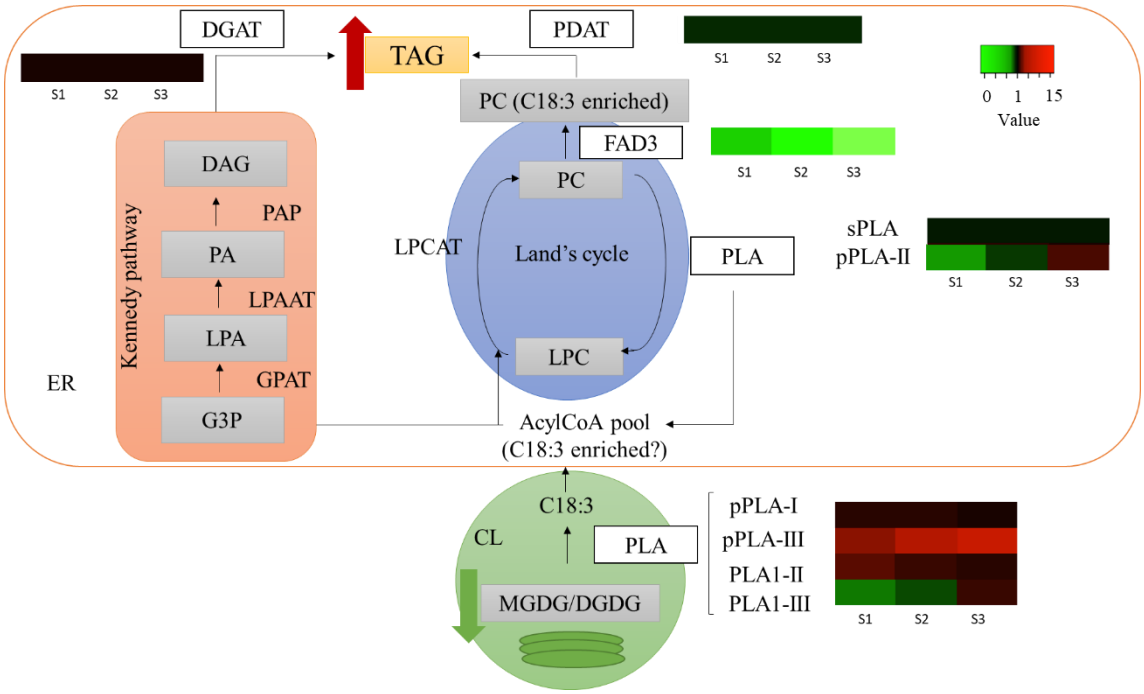

Fig. 17 Schematic model of TAG biosynthesis pathways (Kennedy pathway and Land's cycle) and linolenic acid flow. C, control; S1, moderate stress; S2, severe stress; S3, extreme stress; TAG, triacylglycerol; MGDG, monogalactosyldiacylglycerol; DGDG, digalactosyldiacylglycerol; PLA, phospholipases A; PC, phosphatidylcholine; DGAT, Diacylglycerol Acyltransferase; PDAT, Phospholipid: Diacylglycerol Acyltransferase (PDAT); FAD3, Omega-3 fatty acid Desaturase; DAG, Diacylglycerol; GPAT, glycerol-3-phosphate acyltransferase; G3P, glycerol-3-phosphate; LPAAT, lysophosphatidic acid acyltransferase; LPA, lysophosphatidic acid; PA, phosphatidic acid; PAP, phosphatidic acid phosphatase. Also shown is the gene expression in C, S1, S2 and S3 for the candidate genes for PLA, DGAT, PDAT and FAD3. Adapted from Wang *et al*., 2012a.

6. Conclusion

According to Edgerton (2009) the use of new cultivars with improved drought tolerance will be one of the major needs for agriculture. In the present work, a comprehensive study of soybean lipid metabolism under water stress was conducted. The possible involvement of members of the PLA superfamily in this fatty acid recycling process was addressed in the present work by a combination of physiological, biochemical and molecular assays. Our results suggest that galactolipids relative abundance and their content in linolenic acid decrease through hydrolysis by PLA. PC and neutral lipid content in linolenic acid increases, as well as the relative abundance of neutral lipids indicating that TAG is being produced, through recycling of fatty acids from membrane lipids. We have characterized the PLA gene superfamily in *Glycine max*. PLA is divided in four families, PLA1, PA-preferring PLA1, pPLA and sPLA, comprising a total of 50 genes encoding 55 proteins Among these, a few candidate genes were selected. Other key elements of the metabolic pathways under investigation, PDAT, DGAT and FAD3, were also

studied, which, together with lipid profiling and physiological analyses, provide a comprehensive characterization of the lipid remodelling occurring in drought-stressed soybean leaves. The hypothesis suggested in the present work consisted in the recycling of C18:3 from galactolipids to PC and consequently to TAG, in processes involving PLA but not FAD3. The results obtained support the suggested hypothesis. More studies must be conducted to prove the hypothesis that the studied PLA genes are the responsible ones for TAG accumulation, as well as to ascertain that linolenic acid and PC are involved in TAG accumulation that occur in *Glycine max* leaves under drought stress.

7. References

Akýnci, Ş., & Lösel, D. M. (2012). Plant Water-Stress Response Mechanisms. In I. M. M. R. and H. Hasegawa (Ed.), *Water stress* (pp. 15–42). InTech

Almeida, A. M., Silva, A. B., Araújo, S. S., Cardoso, L. A., Santos, D. M., Torné, Silva, J. M., Paul, M. J., Fevereiro, P. S. (2007). Responses to water withdrawal of tobacco plants genetically engineered with the AtTPS1 gene: a special reference to photosynthetic parameters. *Euphytica*, 113–126. https://doi.org/10.1007/s10681-006-9277-2

Angelopoulos, K., Dichio, B., Xiloyannis, C. (1996). Inhibition of photosynthesis in olive trees (*Olea europaea* L.) during water stress and rewatering. *Journal of Experimental Botany*, 47(301), 1093–1100. https://doi.org/https://doi.org/10.1093/jxb/47.8.1093

Bacelar, E. A., Correia, C. M., Moutinho-Pereira, J. M., Gonçalves, C., Lopes, J. I., Torres-Pereira, J. M. G. (2004). Sclerophylly and leaf anatomical traits of five field-grown olive cultivars growing under drought conditions. *Tree Physiology*, 233–239. https://doi.org/10.1093/treephys/24.2.233

Baker, N.R., Rosenqvist, E. (2004). Applications of chlorophyll fluorescence can improve crop production strategies: an examination of future possibilities. *Journal of Experimental Botany*, 55(403), 1607-1621. https://doi.org/10.1093/jxb/erh196

Bathke, D. (2016). U.S. Drought Monitor. National Drought Mitigation Center, In *United States Department of Agriculture, and National Oceanic and Atmospheric Administration*

Beardsell, M. F., Cohen, D. (1975). Relationships between Leaf Water Status, Abscisic Acid Levels, and Stomatal Resistance in Maize and Sorghum. *Plant Physiology*, 207–212. https://doi.org/https://doi.org/10.1104/pp.56.2.207

Bertolli, S. C., Rapchan, G. L., Souza, G. M. (2012). Photosynthetic limitations caused by different rates of water-deficit induction in *Glycine max* and *Vigna unguiculata*. *Photosynthetica*, 50(3), 329-336. https://doi.org/10.1007/s11099-012-0036-4

Boudière, L., Michaud, M., Petroutsos, D., Rébeillé, F., Falconet, D., Bastien, O., Roy, S., Finazzi, G., Rolland, N., Jouhet, J., Block, M. A., Maréchal, E. (2013). Glycerolipids in photosynthesis : Composition, synthesis and trafficking. *Biochimica et Biophysica Acta*, *1837*, 470–480. https://doi.org/10.1016/j.bbabio.2013.09.007

Caires AR, Scherer MD, Santos TS, Pontim BC, Gavassoni WL, O. S. (2010). Water Stress Response of Conventional and Transgenic Soybean Plants Monitored by Chlorophyll a Fluorescence. *Journal of Fluoresence*, 645–649. https://doi.org/10.1007/s10895-009-0594-4

Chapman, K. D., Ohlrogge, J. B. (2012). Compartmentation of Triacylglycerol Accumulation in Plants. *The Journal of Biological Chemistry*, 287(4), 2288-2294. https://doi.org/10.1074/jbc.R111.290072

Chappelle, E. W., Wood, F. M., McMurtrey, J. E., Newcomb, W. W. (1984). Laser induced fluoresence of green plants. 1: a technique for the remote detection of plant stressand species differentiation. *Applied Optics*, *23*(1), 1–5. https://dx.doi.org/10.1364/AO.23.000134

Chen, G., Greer, M. S., & Weselake, R. J. (2013). Plant phospholipase A : advances in molecular biology, biochemistry, and cellular function. *Biomolecular Concepts*, *4*(5), 527–532. https://doi.org/10.1515/bmc-2013-0011

Duarte, B., Cabrita, M. T., Gameiro, C., Matos, A. R., Godinho, R., Marques, J. C., Cac, I. (2016). Disentangling the photochemical salinity tolerance in *Aster tripolium* L .: connecting biophysical traits with changes in fatty acid composition. *Plant Biology*. Doi: 10.1111/plb.12517

Duarte, B., Santos, D., Marques, J. C., Caçador, I. (2013). Plant Physiology and Biochemistry Ecophysiological adaptations of two halophytes to salt stress : Photosynthesis , PS II photochemistry and anti-oxidant feedback e Implications for resilience in climate change. *Plant Physiology et Biochemistry*, *67*, 178–188. https://doi.org/10.1016/j.plaphy.2013.03.004

Duarte, B., Santos, D., Marques, J. C., Caçador, I. (2015). Estuarine , Coastal and Shelf Science Impact of heat and cold events on the energetic metabolism of the C3 halophyte *Halimione portulacoides*. *Estuarine, Coastal and Shelf Science*, *167*, 166–177. https://doi.org/10.1016/j.ecss.2015.10.003

Edgerton, M. D. (2009). Increasing Crop Productivity to Meet Global Needs for Feed, Food and Fuel. *Plant Physiology*, 149, 7-13. https://doi.org/10.1104/pp.108.130195

Ellinger, D., Stingl, N., Kubigsteltig, I. I., Bals, T., Juenger, M., Pollmann, S., … Germany, D. E. (2010). DONGLE and DEFECTIVE IN ANTHER DEHISCENCE1 Lipases Are Not Essential for Wound- and Pathogen-Induced Jasmonate Biosynthesis : Redundant Lipases Contribute to Jasmonate Formation, *153*(May), 114–127. https://doi.org/10.1104/pp.110.155093

FAOSTAT (2016). *Production/Yield quantities of Soybeans in World*. Food and Agriculture Organization os the United Nations

Farooq, M., Basra, S. M. A., Wahid, A., Ahmad, N., Saleem, B. A. (2009). Improving the Drought Tolerance in Rice (*Oryza sativa* L .) by Exogenous Application of Salicylic Acid. *Journal of Agronomy and Crop Science*, 237–246. https://doi.org/10.1111/j.1439-037X.2009.00365.x

Flexas, J., Barón, M., Bota, J., Ducruet, J., Gallé, A., Galmés, J., Jiménez, M., Pou, A., Ribas-Carbó, M., Sajnani, C., Tomàs, M., Medrano, H. (2009). Photosynthesis limitations during water stress acclimation and recovery in the drought-adapted *Vitis* hybrid Richter-110. *Journal of Experimental Botany*, 60(8), 2361–2377. https://doi.org/10.1093/jxb/erp069

Gameiro, C., Utkin, A. B., Cartaxana, P., Silva, J. M., Matos, A. R. (2016). The use of laser induced chlorophyll fluorescence (LIF) as a fast and non-destructive method to investigate water deficit in *Arabidopsis*. *Agricultural Water Management*, 164, 127-136. https://doi.org/10.1016/j.agwat.2015.09.008

Gascuel, O. (1997). BIONJ: An Improved Version of the NJ Algorithm Based on a Simple Model of Sequence Data. Molecular Biology and Evolution, 685–695. Doi: 14: 685-695

Gasteiger, E., Hoogland, C., Gattiker, A., Duvaud, S., Wilkins, M.R., Appel, R.D., Bairoch A. (2005). Protein identification and analysis tools on the ExPASy Server in *The Proteomics Protocols Handbook*, ed. J. Walker (Humana Press), 571–607. doi:10.1385/1-59259-890-0%3A571

Gasulla, F., Dorp, K. vom, Dombrink, I., Zähringer, U., Gisch, N., Dörmann, P., & Bartels, D. (2013). The role of lipid metabolism in the acquisition of desiccation-tolerance in Craterostigma plantagineum: a comparative approach. *The Plant Journal*, *75*(5), 726–741. https://doi.org/10.1111/tpj.12241

Gigon, A., Matos, A. R. Laffray, D., Zuily-Fodil, Y., Pham-Thi, A. -T. (2004). Effect of Drought Stress on Lipid Metabolism in the Leaves of *Arabidopsis thaliana* (Ecotype Columbia). *Annals of Botaby*, 94(3), 345-351. https://doi.org/10.1093/aob/mch150

Gitelson, A. A., Buschmann, C., & Lichtenthaler, H. K. (1998). Leaf Chlorophyll Fluorescence Corrected for Re-absorption by Means of Absorption and Reflectance Measurements. *Journal of Plant Physiology*, *152*(2–3), 283–296. https://doi.org/10.1016/S0176-1617(98)80143-0

Gupta, P., Saini, R., & Dash, P. K. (2017). Origin and evolution of group XI secretory phospholipase A 2 from flax (*Linum usitatissimum*) based on phylogenetic analysis of conserved domains. *3 Biotech*, *7*(3), 1–10. https://doi.org/10.1007/s13205-017-0790x

Hák, R., Lichtenthaler, H. K., & Rinderle, U. (1990). Decrease of the chlorophyll fluorescence ratio F 690 / F 730 during greening and development of leaves. *Radiation and Environmental Biophysics*, 329–336. https://doi.org/https://doi.org/10.1007/BF01210413

Heath R, Packer L. (1968). Photoperoxidation in isolated chloroplasts. I. Kinetics and stoichiometry of fatty acid peroxidation. *Archives in Biochemistry and Biophysics*, 125,189–198. Doi: 10.1016/0003-9861(68)90654-1

Hellemans, J., Mortier, G., Paepe, A., Speleman, F., Vandesompele, J. (2007). qBase relative quantification framework and software for management and automated analysis of real-time quantitative PCR data. *Genome Biology*, 8(2). https://doi.org/10.1186/gb-2007-8-2-r19

Holk, A., Rietz, S., Zahn, M., Quader, H., & Scherer, G. F. E. (2002). Molecular Identification of Cytosolic , Patatin-Related Phospholipases A from Arabidopsis with Potential Functions in Plant Signal Transduction 1. *Plant Physiology*, *130*(September), 90–101. https://doi.org/10.1104/pp.006288.90

Hölzl, G., Witt, S., Gaude, N., Melzer, M., Scho, M. A., Dörmann, P. (2009). The Role of Diglycosyl Lipids in Photosynthesis and Membrane Lipid Homeostasis in Arabidopsis. *Plant Physiology*, *150*(July), 1147–1159. https://doi.org/10.1104/pp.109.139758

Ishiguro, S., Kawai-oda, A., Ueda, J., Nishida, I., & Okada, K. (2001). The DEFECTIVE IN ANTHER DEHISCENCE1 Gene Encodes a Novel Phospholipase A1 Catalyzing the Initial Step of Jasmonic Acid Biosynthesis , Which Synchronizes Pollen Maturation , Anther Dehiscence , and Flower Opening in Arabidopsis. *The Plant Cell*, *13*(October), 2191–2209

Jaleel, C. A., Manivannan, P., Wahid, A., Farooq, M., Al-Juburi, H. J., Somasundaram, R., & Panneerselvam, R. (2009). Drought Stress in Plants : A Review on Morphological Characteristics and Pigments Composition. *International Journal of Agriculture & Biology*, 100–105

Katoh, K., & Standley, D. M. (2013). MAFFT Multiple Sequence Alignment Software Version 7 : Improvements in Performance and Usability. *Molecular Biology and Evolution*, *30*(4), 772–780. https://doi.org/10.1093/molbev/mst010

Kaup, M.T, Froese,C.D. Thompson, G.E. (2002) A Role for Diacylglycerol Acyltransferase during Leaf Senescence. *Plant Physiology*. 129(4): 1616–1626

Kennedy, E. P., & Weiss, S. B. (1956). The function of cytidine coenzymes in the biosynthesis of phospholipids. *The Journal of Biological Chemistry*, *222*(1), 193–214

Ku, Y.-S., Au-Yeung, W.-K., Yung, Y.-L., Li, M.-W., Wen, C.-Q., Liu, X., & Lam, H.-M. (2013). Drought Stress and Tolerance in Soybean. In J. E. Board (Ed.), *Comprehensive Survey of International Soybean Research - Genetics, Physiology, Agronomy and Nitrogen Relationships*. InTech. https://doi.org/http://dx.doi.org/10.5772/52945

Lands, E. M. (1960). Metabolism of Glycerolipids II. The enzymatic acylation of lysolecithin. *The Journal of Biological Chemistry*, *235*(8)

Le, D. T., Nishiyama, R. Watanabe, Y. Tanaka, M., Seki, M., Ham, L. H., Yamaguchi-Shinozaki, K., Shinozaki, K., Tran, L. P. (2012). Differential Gene Expression in Soybean Leaf Tissues at Late Developmental Stages under Drought Stress Revealed by Genome-Wide Transcriptome Analysis. *Plos One*, 7(11). https://doi.org/10.1371/journal.pone.0049522

Lee, H. Y., Bahn, S. C., Shin, J. S.,Hwang, I.; Back, K., Doelling, J. H., Ryu, S. B. (2005). Multiple forms of secretory phospholipase A2 in plants. *Progress in Lipid Research*, *44*, 52–67. https://doi.org/10.1016/j.plipres.2004.10.002

Leekumjorn, S., Cho, H. J., Wu, Y., Wright, N. T., Sum, A. K., Chan, C. (2009). The Role of Fatty Acid Unsaturation in Minimizing Biophysical Changes on the Structure and Local Effects of Bilayer Membranes. *Biochimica et Biophysica Acta*, 1788(7), 1508–1516. https://doi.org/10.1016/j.bbamem.2009.04.00

Lepage, M. (1967). Identification and Composition of Turnip Root Lipids. *Lipids*, 244-250. https://doi.org/10.1007/BF02532563

Li, M., Bahn, S. C., Guo, L., Musgrave, W., Berg, H., Welti, R., Wang, X. (2011). Patatin-Related Phospholipase pPLAIII b -Induced Changes in Lipid Metabolism Alter Cellulose Content and Cell Elongation in *Arabidopsis*. *The Plant Cell*, *23*(March), 1107–1123. https://doi.org/10.1105/tpc.110.081240

Li, R., Hatanaka, T., Yu, K., Wu, Y., Fukushinge, H., Hildebrand, D. (2013). Soybean oil biosynthesis: role of diacylglycerol acyltransferases. *Functional and Integrative Genomics*, 13(1), 99–113. Doi: 10.1007/s10142-012-0306-z

Lichtenthaler, H. K. (1987). Chlorophylls Carotenoids. *Methods in Enzimology*, *148*, 350–382. https://doi.org/https://doi.org/10.1016/0076-6879(87)48036-1

Lisar, S. Y. S., Motafakkerazad, R., Hossain, M. M., Rahman, I. M. M. (2012). Water Stress in Plants: Causes, Effects and Responses. In I. M. M. R. and H. Hasegawa (Ed.), *Water stress*. In. https://doi.org/10.5772/1419

Liu, Q., Sun, Y., Chen, J., Li, P., Li, C., Niu, G., Jiang, L. (2016). Transcriptome analysis revealed the dynamic oil accumulation in *Symplocos paniculate* fruit. *BMC Genetics*, 1-17. https://doi.org/10.1186/s12864-016-3275-0

Lu, C., Zhang, J. (1999). Effects of water stress on photosystem II photochemistry and its thermostability in wheat plants. *Journal of Experimental Botany*, 50(336), 1199–1206. https://doi.org/https://doi.org/10.1093/jxb/50.336.1199

Machado, A., Arrabaça, J. D., Matos, A. R. (2013) Phospholipases A in soybean: gene identification and expression in response to drought. *XIII Congresso Luso-Espanhol de Fisiologia Vegetal*, Lisbon, Faculdade de Ciências de Lisboa.

Machado, A., Arrabaça, J. D., Matos, A. R. (2013) Searching for drought-induced phospholipase A genes: a comparative analysis between Soybean and Arabidopsis. *Plant Symposium Oxidative stress and cell death in plants*: mechanisms and implications.

Manavalan, L. P., Guttikonda, S. K., Tran, L. P., Nguyen, H. T. (2009). Physiological and Molecular Approaches to Improve Drought Resistance in Soybean. *Plant Cell Physiology*, *50*(7), 1260–1276. https://doi.org/10.1093/pcp/pcp082

Mansfeld, J., & Ulbrich-Hofmann, R. (2007). Secretory phospholipase A2-α from *Arabidopsis thaliana*: functional parameters and substrate preference. *Chemistry and Physics of Lipids*, *150*, 156–166. https://doi.org/10.1016/j.chemphyslip.2007.07.001

Marcolino-Gomes, J., Fabiana, A. R., Fuganti-Pagliarini, R., Nakayama, T. J., Reis, R. R., Fatias, J. R. B., Harmon, F. G., Molinari, B. C., Molinari, H., Correa, M. D., Nepomuceno, A. (2015). Transcriptome-Wide Identification of Reference Genes for Expression Analysis of Soybean Responses to Drought Stress along the Day. *Plos One*, 1-16. https://doi.org/10.1371/journal.pone.0139051

Mariani, M. E., Villarreal, M. A., Cheung, F., Leiva, E. P. M., Madoery, R. R., & Fidelio, G. D. (2012). In silico and in vitro characterization of phospholipase A 2 isoforms from soybean (*Glycine max*). *Biochimie*, *94*(12), 2608–2619. https://doi.org/10.1016/j.biochi.2012.07.021

Martin, B. A., Schoper, J. B., Rinne, R. W. (1986). Changes in Soybean (*Glycine max* [L . J Merr .) Glycerolipids in Response to Water Stress. *Plant Physiology*, *81*, 798–801. Doi: 0032-0889/86/81/0798/04/$01.00/0

Martynenko, A., Shotton, K., Astatkie, T., Petrash, G., Fowler, C., Neily, W., Critchley, A. T. (2016). Thermal imaging of soybean response to drought stress : the effect of Ascophyllum nodosum seaweed extract. *SpringerPlus*. https://doi.org/10.1186/s40064-016-3019-2

Matos, A. R., D'Arcy-Lameta, A., França, M., Pêtres, S., Edelman, L., Kader, J.-C., … Pham-Thi, A. T. (2001). A novel patatin-like gene stimulated by drought stress encodes a galactolipid acyl hydrolase. *FEBS Letters*, *491*, 188–192

Matos, A. R., Gigon, A., Laffray, D., Pêtres, S., Zuily-Fodil, Y., Pham-Thi, A. -T. (2008). Effects of progressive drought stress on the expression of patatin-like lipid acyl hydrolase genes in *Arabidopsis* leaves. *Physiologia Plantarum*, 134(1), 110-120. https://doi.org/10.1111/j.1399-3054.2008.01123.x

Matos, A. R., Pham-Thi, A., -T. (2009). Lipid deacylating enzymes in plants: Old activities, new genes. *Plant Physiology and Biochemistry*, 47(6), 491-503. https://doi.org/10.1016/j.plaphy.2009.02.011

Matsui, K., Fukutomi, S., Ishii, M., Kajiwara, T. (2004). A tomato lipase homologous to DAD1 (LeLID1) is induced in post-germinative growing stage and encodes a triacylglycerol lipase. *Federation of European Biochemical Societies*, 569, 195–200. https://doi.org/10.1016/j.febslet.2004.05.064

Monteiro de Paula, F., Pham-Thi, A. T., Silva, J. V. da, Justin, A. M., Demandre, C., & Mazliak, P. (1990). Effects of water stress on the molecular species composition of polar lipids from *Vigna unguiculata* L. Leaves. *Plant Science*, *66*, 185–193. https://doi.org/https://doi.org/10.1016/0168-9452(90)90203-Z

Morgan, J. M. (1984). Osmoregulation and Water Stress in Higher Plants, (30), 299–319. https://doi.org/10.1146/annurev.pp.35.060184.001503

Munnik, I., Testerink, C. (2008) Plant phospholipid signaling "in a nutshell". The Journal of Lipid Research (50). doi: 10.1194/jlr.R800098-JLR200

Nouairi, I., Ammar, W. Ben, Youssef, N. Ben, Miled, D. D. Ben, Ghorbal, M. H., Zarrouk, M. (2009). Antioxidant defense system in leaves of Indian mustard (*Brassica juncea*) and rape (*Brassica napus*) under cadmium stress. *Acta Physiologiae Plantarum*, *31*(2), 237–247. https://doi.org/10.1007/s11738-008-0224-9

Ohashi, Y., Nakayama, N., Saneoka, H., Fujita, K. (2006). Effects of drought stress on photosynthetic gas exchange , chlorophyll fluorescence and stem diameter of soybean plants. *Biologia Plantarum*, *50*(1), 138–141. https://doi.org/https://doi.org/10.1007/s10535-005-0089-3

Osakabe, Y., Osakabe, K., Shinozaki, K., & Tran, L.-S. P. (2014). Response of plants to water stress. *Frontiers in Plant Science*, *5*(March), 1–8. https://doi.org/10.3389/fpls.2014.00086

Páli, T., Garab, G., Horváth, L. I., Kóta, Z. (2003). Functional significance of the lipid-protein interface in photosynthetic membranes. *Cellular and Molecular Life Sciences*, *60*, 1591–1606. https://doi.org/10.1007/s00018-003-3173-x

Peleg, Z., Blumwald, E. (2011). Hormone balance and abiotic stress tolerance in crop plants. *Current Opinion in Plant Biology*, 14(3), 290–295. https://doi.org/10.1016/j.pbi.2011.02.001

Pettai, H., Oja, V., Freiberg, A., Laisk, A. (2005). Photosynthetic activity of far-red light in green plants. *Biochimica et Biophysica Acta (BBA) - Bioenergetics*, *1708*, 311–321. https://doi.org/10.1016/j.bbabio.2005.05.005

Pham-Thi, A. -T., Borrel-Flood, C., Silva, J. V. da, Justin, A. M., & Mazliak, P. (1985). Effects of water stress on lipid metabolism in cotton leaves. *Phytochemistry*, 24(4), 123–127. https://doi.org/https://doi.org/10.1016/S0031-9422(00)84884-0

Pham-Thi, A. -T., Vieira, J., Silva, D., Mazliak, P. (1990). The role of membrane lipids in drought resistance of plants. *Bulletin de La Société Botanique de France*. https://doi.org/10.1080/01811789.1990.10826991

Purcell, L. C., King, C. A., & Ball, R. A. (2014). Soybean Cultivar Differences in Ureides and the Relationship to Drought Tolerant Nitrogen Fixation and Manganese Nutrition. *Crop Science*, (ii), 1062–1070

Repellin, A., Pham-Thi, A. T., Tashakorie, A., Sahsah, Y., Daniel, C., & Zuily-Fodil, Y. (1997). Leaf membrane lipids and drought tolerance in young coconut palms (Cocos nucifera L .). *European Journal of Agronomy*, 6, 25–33. https://doi.org/10.1016/S1161-0301(96)02034-5

Richmond, G. S., Smith, T. K. (2011). Phospholipases A1. *International Journal of Molecular Sciences*, 588–612. https://doi.org/10.3390/ijms12010588

Ryu, S. B. (2004). Phospholipid-derived signalling mediated by phospholipase A in plants. *Trends in Plant Science*, 985). https://doi.org/10.1016/j.tplants.2004.03.004

Sah, S. K., Reddy, K. R., & Li, J. (2016). Abscisic Acid and Abiotic Stress Tolerance in Crop Plants. *Frontiers in Plant Science*, *7*(May), 1–26. https://doi.org/10.3389/fpls.2016.00571

Sanda, S., Yoshida, K., Kuwano, M., Kawamura, T., Nakajima, Y. (2011). Responses of the photosynthetic electron transport system to excess light energy caused by water deficit in wild watermelon. *Physiologia Plantarum*, 247–264. https://doi.org/10.1111/j.1399-3054.2011.01473.x

Scherer, F. E., Ryu, S. B., Wang, X., Matos, A. R., Heitz, T. (2010). Patatin-related phospholipase A : nomenclature , subfamilies and functions in plants. *Trends in Plant Science*, *15*(12), 693–700. https://doi.org/10.1016/j.tplants.2010.09.005

Schmidt, C. W. (2007). Biodiesel - Cultivating Alternative Fuels. *Environmental Health Perspectives*, *115*(2)

Sinclair, T. R., Purcell, L. C., King, C. A., Sneller, C. H., Chen, P., & Vadez, V. (2007). Drought tolerance and yield increase of soybean resulting from improved symbiotic N2 fixation. *Field Crops Research*, *101*, 68–71. https://doi.org/10.1016/j.fcr.2006.09.010

Singh, A., Baranwal, V., Shankar, A., Kanwar, P., Ranjan, R., & Yadav, S. (2012). Rice Phospholipase A Superfamily : Organization , Phylogenetic and Expression Analysis during Abiotic Stresses and Development. *PLOS ONE*, *7*(2). https://doi.org/10.1371/journal.pone.0030947

Souza, G. M., Catuchi, T. A., Bertolli, S. C., Soratto, R. P. (2013). Soybean Under Water Deficit: Physiological and Yield Responses. In James E. Board (Ed.), *A Comprehensive Survey of International Soybean Research – Genetics, Physiology, Agronomy and Nitrogen Relationships* (pp. 273-298). Rijeka, Croatia: InTech. https://doi.org/10.5772/54269

Torres-Franklin, M. -L., Gigon, A., Melo, D. F., Zuily-Fodil, Y., Pham-Thi, A. -T. (2007). Drought stress and rehydration affect the balance between MGDG and DGDG synthesis in cowpea leaves. *Physiologia Plantarum*, 131(2), 201-210. https://doi.org/10.1111/j.1399-3054.2007.00943.x

Torres-Franklin, M. -L., Repellin, A., Huynh, V., Arcy-Lameta, A., Zuily-Fodil, Y., Pham-Thi, A. -T. (2009). Omega-3 fatty acid desaturase (*FAD3, FAD7, FAD8*) gene expression and linolenic acid content in cowpea leaves submitted to drought and after rehydration. *Environmental and Experimental Botany*, 65, 162-169. https://doi.org/10.1016/j.envexpbot.2008.12.010

United Nations (2010). United Nations Decade 2010 – 2020 for deserts and the fight against desertification

USDA (2017). *U.S. Bioenergy Statistics: Biodiesel supply and disappearance*. United States Department of Agriculture – Economic Research Service

Vandesompele, J., Preter, K., Pattyn, F., Poppe, B., Van Roy, N., Paepe, A., Speleman, F. (2002). Accurate normalization of real-time quantitative RT-PCR data by geometric averaging of multiple internal control genes. *Genome Biology*, 1-12. https://doi.org/10.1186/gb-2002-3-7-research0034

Verlotta, A., Liberatore, M. T., Cattivelli, L., Trono, D. Secretory Phospholipases A2 in Durum Wheat (*Triticum durum* Desf.): Gene Expression, Enzymatic Activity and Relation to Drought Stress Adaptation. *International Journal of Molecular Sciences*, 5146–5169. https://doi.org/10.3390/ijms14035146

Wang, F., Deng, Y., Zhou, Y., Dong, J., Chen, H., Dong, Y., … Li, H. (2015). Genome-Wide Analysis and Expression Profiling of the Phospholipase C Gene Family in Soybean (*Glycine max*). *PLOS ONE*. https://doi.org/10.1371/journal.pone.0138467

Wang, L., Shen, W., Kazachkov, M., Chen, G., Chen, Q., Carlsson, A. S., Stymne, S., Weselake, R. J., Zou, J. (2012) a. Metabolic Interactions between the Lands Cycle and the Kennedy Pathway of Glycerolipid Synthesis in Arabidopsis Developing Seeds. *The Plant Cell*, *24*, 4652–4669. https://doi.org/10.1105/tpc.112.104604

Wang, Z. X., Chen, L., Ai, J., Qin, H. Y., Liu, Y. X., Xu, P. L., Jiao, Z. Q., Zhao, Y., Zhang, Q. T. b (2012) b. Photosynthesis and activity of photosystem II in response to drought stress in Amur Grape (*Vitis amurensis* Rupr.). *Photosynthetica*, *50*(2), 189–196. https://doi.org/10.1007/s11099-012-0023-9

Wang, X. (2001). Plant phospholipases. *Annual Review of Plant Physiology*, *2*. https://doi.org/10.1146/annurev.arplant.52.1.21

Weselake, R. J., Shah, S., Tang, M., Quant, P. A., Snyder, C. L., Furukawa-Stoffer, T. L., Zhu, W., Taylor, D. C., Zou, J., Kumar, A., Hall, L., Laroche, A., Rakow, G., Raney, P., Moloney, M. M., Harwood, J. L. (2008). Metabolic control analysis is helpful for informed genetic manipulation of oilseed rape (*Brassica napus*) to increase seed oil content. *Journal of Experimental Botany*, 59(13), 3543-3549. https://doi.org/10.1093/jxb/ern206

Yuan, X. K., Yang, Z. Q., Li, Y. X., Liu, Q., Han, W. (2016). Effects of different levels of water stress on leaf photosynthetic characteristics and antioxidant enzyme activities of greenhouse tomato. *Photosynthetica*, *53*(2014), 1–13.https://doi.org/10.1007/s11099-015-0122-5

Zhang, H. T., Bi, Y. P., Liu, Z. J., Shan, L. (2009). Heterologous Expression of Two Glycine max ω – 3 Fatty Acid Desaturases in *Saccharomyces cerevisiae*. *Russian journal of Plant Physiology*, 56(4), 629-634. https://doi.org/10.1134/S1021443709040189

Zhang, Y. J., Xie, Z. K., Wang, Y. J., Su, P. X., An, L. P., Gao, H., Land, S. (2011). Effect of Water Stress on Leaf Photosynthesis , Chlorophyll Content , and Growth of Oriental Lily. *Russian Journal of Plant Physiology*, *58*(5), 844–850. https://doi.org/10.1134/S1021443711050268

Zhao, J., Zhou, D., Zhang, Q., & Zhang, W. (2012). Genomic analysis of phospholipase D family and characterization of GmPLD in soybean (Glycine max). *Journal of Plant Research*, 569–578. https://doi.org/10.1007/s10265-011-0468-0

8. Supplementary data

8.1. Supplementary data 1

Supplementary data 1. Target genes information for qPCR. Represented are primer sequences, annealing temperature (Ta) amplicon size (bp), amplification efficiency and average control Ct of the genes *GmsPLA2-αI, GmpPLA-IαII, GmpPLA-IIαIa, GmpPLA-IIIαII, GmPLA1-IIγa, GmPLA1-III*, *GmDGAT1C*, *GmPDAT1E* and *GmFAD3C.* FW, Forward; RV, Reverse.

	ID	Primer sequences (5'-3')	Ta (ºC)	Amplicon size (bp)	Amplification efficiency	Control average Ct (± SD)
Reference genes	*Golgin-84* (Glyma.08G053300.1)	FW: ATGAGAAGTTTTCGTAGCCT RV: TTGGGGTTATGAATGCTGT	54	138	2.07	26.5 ± 0.1
Reference genes	*NUDIX* (Glyma.13G171900.1)	FW: TCGTAGCAGCCAGAGTTCTA RV: TGGGATGGCATTCAATAGGT	60	114	1.91	18.8 ± 0.1
$sPLA_2$	*GmsPLA2-αI* (Glyma.07G129900.1)	FW: GCCCCCTCATTCAAGTATG RV: CCACTATACAAAAGTCCACAG	58	209	1.92	22.9 ± 0.1
pPLA - I	*GmpPLA-IαII* (Glyma.07G259000.1)	FW: GTTGTTTCCGATGTTCCTTAC RV: TACTCCGAAGCCCTAATCC	60	96	1.96	29.6 ± 0.1
pPLA - II	*GmpPLA-IIαIa* (Glyma.14G081300.1)	FW: TGCTCTCACAGAAGACAAATC RV: TACTGGTGCAGAGAATCTAAG	60	148	2.02	30.3 ± 0.2
pPLA - III	*GmpPLA-IIIαII* (Glyma.10G211300.1)	FW: CTGCTTCAAAGGAACTGT RV: GGTCAGAGACAAGTATGG	54	85	1.90	25.8 ± 0.7
PLA1-II	*GmPLA1-IIγa* (Glyma.13G231100.1)	FW: AGGTTGTTGTCGATTGGAGA RV: GATTATCGCGTGAGGCTTCT	60	119	2.08	27.2 ± 0.3
PLA1-III	*GmPLA1-III* (Glyma.08G100400.1)	FW: GCACTCAACTCCAACCAT RV: ACGTAACCACGGCTGAAG	56	109	1.92	28.6 ± 0.3
DGAT	*GmDGAT1C* (Glyma.09G065300.1)	FW: GATCTCCGACAGCCTTCTC RV: TGTCGTCGTCGGTGATTTTG	60	112	1.91	25.3 ± 0.7
PDAT	*GmPDAT1E* (Glyma.12G084000.1)	FW: TCAATGTACGTGTATGGG RV: ATGCTGCTTCAGATGAGTCAC	54	73	1.89	26.1 ± 0.2
FAD3	*GmFAD3C* (Glyma.18G062000.1)	FW: ATGGCCATGTTGAGAAGGAT RV: CAAAGATGGGGAAAGGAAGA	60	111	1.89	26.1 ± 0.1

8.2. Supplementary data 2

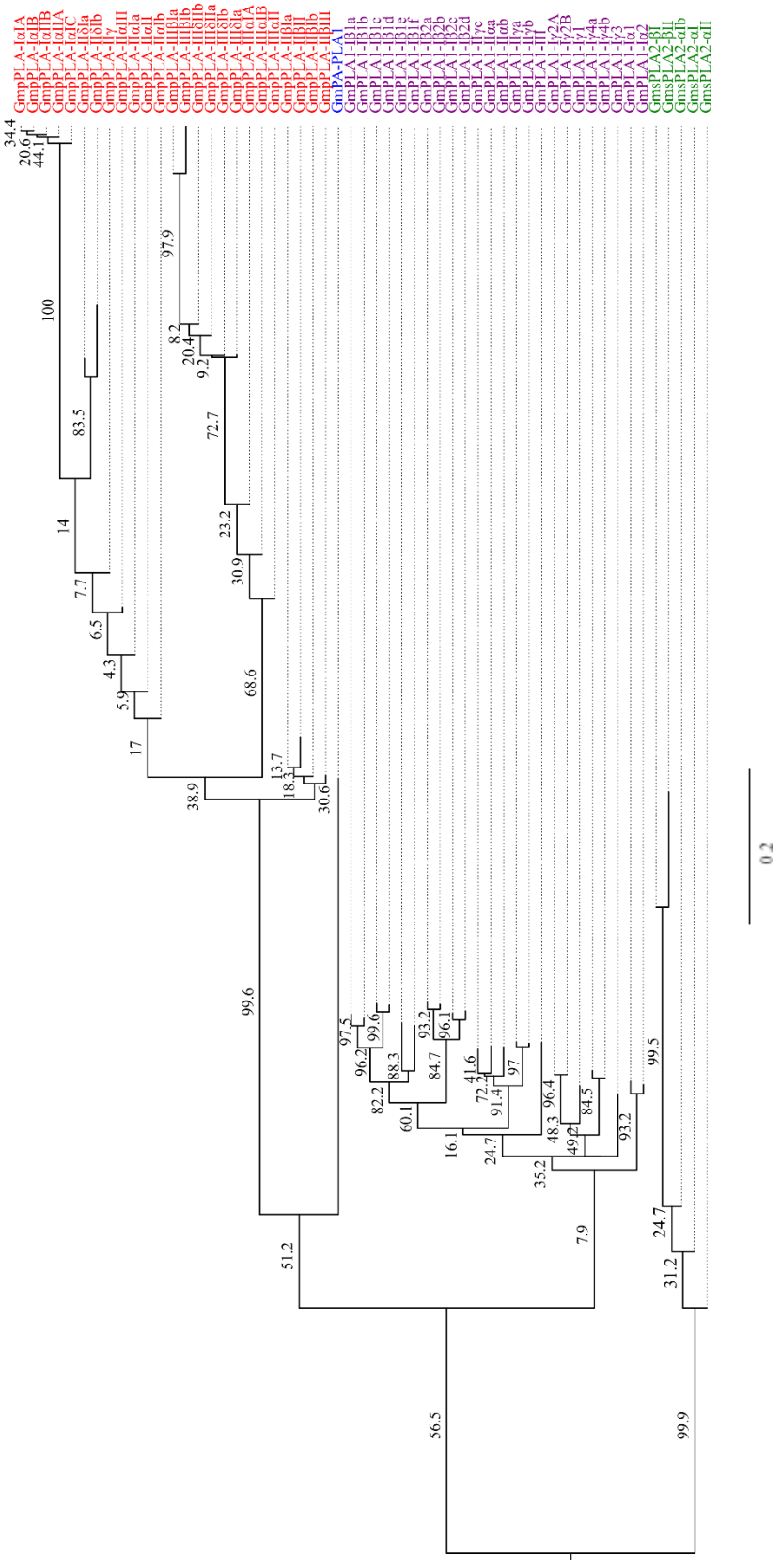

Supplementary data 2. Phylogenetic relationship among various classes of PLA superfamily in *Glycine max*. A rooted BioNJ based tree was generated from the protein sequences of all the PLA classes of soybean. Multiple sequence alignment was done using Clustal W and tree was generated using MegAlign Bootstrap value, out of 1000 replicates is indicated at each node. Scale bar represents 9.0 amino acid substitutions per 100 residues. Coloured in red, blue, purple and green are, respectively, pPLAs, PA-preferring PLA1s, PLA1 and sPLAs.

8.3. Supplementary data 3

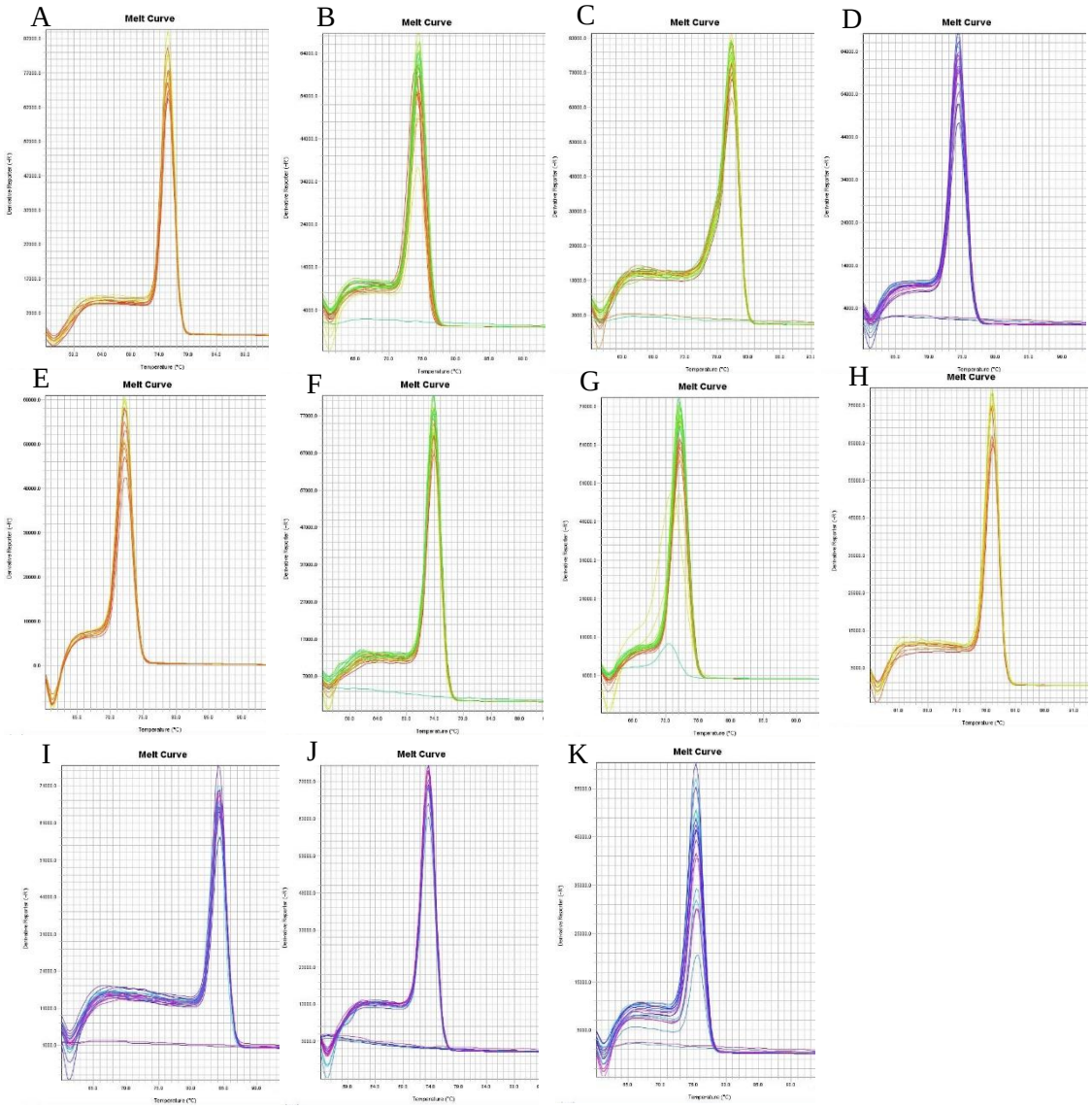

Supplementary data 3: Melting curves of the target genes. (A) Reference gene *Golgin-84*; (B) Reference gene *Nudix*; (C) *GmsPLA2-αI*; (D) *GmpPLA-IαII;* (E) *GmpPLA-IIαIa*; (F) *GmpPLA-IIIαII*; (G) *GmPLA1-IIγa*; (H) *GmPLA1-III*; (I) *GmDGAT1C*; (J) *GmPDAT1E*; (K) *GmFAD3C*.

8.4 Supplementary data 4

Supplementary data 4: General features of *Glycine max* PLA superfamily. Proposed protein nomenclature, Phytozome accession, proposed gene nomenclature, gene locus, nucleotide and protein NCBI accessions, EST, exon-intron number, protein length, molecular weight, pI, domains and prediction of subcellular location are represented. [a]Subcellular location from TargetP v1.1, others are from WoLF PSORT; studied genes are denoted in bold

PLA group	Proposed nomenclature[c]	Phytozome *Glycine max* Wm82.a2.v1 gene locus	Proposed gene nomenclature	NCBI ID_ Gycine_max_v2.0			EST	Exons	Introns	Length (aa)	Mol Wt. (Da)	pI	Domais (Pfam)					Subcellular location (WoLF PSORT/TargetP 1.1)
				Gene Locus	Nucleotide	Protein							LRR 8	Arm	Patatin	Lipase 3	DDHD	
pPLA-I	**GmpPLA-IαIIA**	**Glyma.07G259000**	***GmpPLA-IαII***	**LOC100788345**	**XM_003528632.3**	**XP_003528680.1**	**59**	**19**	**18**	**1332**	**147573**	**5.72**	**1**	**1**	**1**	**0**	**0**	**Chloroplast**
pPLA-I	**GmpPLA-IαIIB**				**XM_014778256.1/XM_014778255.1**	**XP_014633742.1/XP_014633741.1**		**19**	**18**	**1090**	**121373**	**5.89**	**1**	**1**	**1**	**0**	**0**	**Chloroplast/Mitochondria[a]**
pPLA-I	GmpPLA-IαIC	Glyma.17G015200	*GmpPLA-Iα1*	LOC100818519	XM_006600250.2	XP_006600313.1	45	18	17	1292	143149	5.77	1	1	1	0	0	Chloroplast
pPLA-I	GmpPLA-IαIA				XM_003550452.3	XP_003550500.1		18	17	1333	147657	5.8	1	1	1	0	0	Chloroplast
pPLA-I	GmpPLA-IαIB				XM_014769905.1	XP_014625391.1		18	17	1090	121365	5.97	1	1	1	0	0	Chloroplast/Mitochondria[a]
pPLA-II	GmpPLA-IIαIII	Glyma.06G037900	*GmpPLA-IIαIII*	LOC100783909	XM_003527665.3	XP_003527713.1	0	6	5	414	45813	5.96	0	0	1	0	0	Chloroplast/Other[a]
pPLA-II	**GmpPLA-IIαIa**	**Glyma.14G081300**	***GmpPLA-IIαIa***	**LOC100777122**	**XM_003544404.3**	**XP_003544452.1**	**7**	**7**	**6**	**408**	**45243**	**5.97**	**0**	**0**	**1**	**0**	**0**	**Cytosol/Other[a]**
pPLA-II	GmpPLA-IIαII	Glyma.17G244000	*GmpPLA-IIαII*	LOC100798783	XM_003549357.3	XP_003549405.1	1	7	6	409	45083	6.33	0	0	1	0	0	Extracellular/Other[a]
pPLA-II	GmpPLA-IIαIb	Glyma.17G243900	*GmpPLA-IIαIb*	-	-	KRH05706.1	0	7	6	376	41844	5.83	0	0	1	0	0	Extracellular/Other[a]
pPLA-II	GmpPLA-IIβIa	Glyma.14G081200	*GmpPLA-IIβIa*	LOC100776229	XM_003544403.3	XP_003544451.1	3	7	6	408	44911	6.27	0	0	1	0	0	Cytosol/Other[a]
pPLA-II	GmpPLA-IIβIb	Glyma.14G081500	*GmpPLA-IIβIb*	LOC100777639	XM_003544405.3	XP_003544453.1	3	7	6	408	44939	6.27	0	0	1	0	0	Cytosol/Other[a]
pPLA-II	GmpPLA-IIβII	Glyma.17G244100	*GmpPLA-IIβII*	-	-	KRH05708	0	6	5	377	41841	7.71	0	0	1	0	0	Cytosol/Other[a]
pPLA-II	GmpPLA-IIβIII	Glyma.17G244200	*GmpPLA-IIβIII*	LOC100799835	XM_006601230.2	XP_006601293.1	7	7	6	408	44828	6.57	0	0	1	0	0	Cytosol/Other[a]
pPLA-II	GmpPLA-IIγ	Glyma.11G056900	*GmpPLA-IIγ*	LOC100812523	XM_003538767.3	XP_003538815.1	0	7	6	403	44090	6.34	0	0	1	0	0	Cytosol/Other[a]
pPLA-II	GmpPLA-IIδIa	Glyma.07G115500	*GmpPLA-IIδIa*	LOC100802114	NM_001255207.1	NP_001242136.1	14	7	6	418	46170	5.41	0	0	1	0	0	Chloroplast/Secretory pathway[a]
pPLA-II	GmpPLA-IIδIb	Glyma.07G115400	*GmpPLA-IIδIb*	LOC100802647	XM_003528983.3	XP_003529031.1	23	7	6	407	45307	6.11	0	0	1	0	0	Chloroplast/Secretory pathway[a]
pPLA-III	**GmpPLA-IIIαII**	**Glyma.10G211300**	***GmpPLA-IIIαII***	**LOC100818727**	**XM_006589368.2**	**XP_006589431.1**	**13**	**4**	**3**	**463**	**50067**	**6.2**	**0**	**0**	**1**	**0**	**0**	**Chloroplast/Other[a]**
pPLA-III	GmpPLA-IIIαIA	Glyma.20G179600	*GmpPLA-IIIα1*	LOC100815051	XM_003556183.3	XP_003556231.2	12	4	3	544	59940	8.99	0	0	1	0	0	ER/Mitochondria[a]
pPLA-III	GmpPLA-IIIαIB				XM_006606181.2	XP_006606244.1		4	3	462	49856	6.49	0	0	1	0	0	ER/Other[a]
pPLA-III	GmpPLA-IIIβIa	Glyma.09G022000	*GmpPLA-IIIβIa*	LOC100800037	XM_003535011.3	XP_003535059.1	5	2	1	434	46744	8.77	0	0	1	0	0	Cytosol/Other[a]
pPLA-III	GmpPLA-IIIβIb	Glyma.15G128300	*GmpPLA-IIIβIb*	LOC100802299	XM_014767386.1	XP_014622872.1	9	3	2	436	46893	8.88	0	0	1	0	0	Chloroplast/Other[a]
pPLA-III	GmpPLA-IIIδIa	Glyma.02G147100	*GmpPLA-IIIδIa*	LOC100795441	XM_003518875.3	XP_003518923.1	4	2	1	379	41319	8.8	0	0	1	0	0	Chloroplast/Other[a]
pPLA-III	GmpPLA-IIIδIb	Glyma.10G026800	*GmpPLA-IIIδIb*	LOC100777557	XM_003536481.3	XP_003536529.1	16	2	1	380	41481	8.03	0	0	1	0	0	Chloroplast/Other[a]
pPLA-III	GmpPLA-IIIδIIa	Glyma.03G154200	*GmpPLA-IIIδIIa*	LOC100806989	XM_003520522.3	XP_003520570.2	2	2	1	400	44050	8.59	0	0	1	0	0	Chloroplast/Other[a]
pPLA-III	GmpPLA-IIIδIIb	Glyma.19G156700	*GmpPLA-IIIδIIb*	LOC100784729	XM_014771383.1	XP_014626869.1	8	2	1	382	41637	8.61	0	0	1	0	0	ER/Other[a]
PLA1-I	GmPLA$_1$-Iα1	Glyma.18G299300	*GmPLA$_1$-Iα1*	LOC100820494	XM_003551807.2	XP_003551855.1	0	1	0	499	55835	7.24	0	0	0	1	0	Chloroplast
PLA1-I	GmPLA$_1$-Iα2	Glyma.08G362700	*GmPLA$_1$-Iα2*	LOC100803183	XM_003530859.3	XP_003530907.1	0	1	0	489	54495	8.62	0	0	0	1	0	Chloroplast
PLA1-I	GmPLA$_1$-Iγ1	Glyma.02G142200	*GmPLA$_1$-Iγ1*	LOC100779676	XM_003518846.2	XP_003518894.2	5	3	2	530	59701	6.8	0	0	0	1	0	Chloroplast
PLA1-I	GmPLA$_1$-Iγ2A	Glyma.03G159000	*GmPLA$_1$-Iγ2*	LOC100815007	XM_006576857.2	XP_006576920.2	92	3	2	422	47561	6.37	0	0	0	1	0	Chloroplast
PLA1-I	GmPLA$_1$-Iγ2B				XM_006576856.2	XP_006576919.2		3	2	497	56402	6.24	0	0	0	1	0	Chloroplast

PLA1-I	GmPLA$_1$-Iγ4a	Glyma.02G142100	*GmPLA$_1$-Iγ4a*	LOC100779151	XM_003518845.3	XP_003518893.1	10	3	2	466	53060	6.18	0	0	0	1	0	Chloroplast
PLA1-I	GmPLA$_1$-Iγ4b	Glyma.02G141900	*GmPLA$_1$-Iγ4b*	LOC100778615	XM_003518844.3	XP_003518892.1	18	3	2	465	53042	5.96	0	0	0	1	0	Chloroplast
PLA1-I	GmPLA$_1$-Iγ3	Glyma.11G093400	*GmPLA$_1$-Iγ3*	LOC100795661	XM_003538889.3	XP_003538937.1	3	1	0	505	57719	6.42	0	0	0	1	0	Nucleus/Chloroplast[a]
PLA1-I	GmPLA$_1$-Iβ1e	Glyma.03G110600	*GmPLA$_1$-Iβ1e*	LOC100788424	XM_003520377.2	XP_003520425.1	0	1	0	429	48518	9.29	0	0	0	1	0	Chloroplast
PLA1-I	GmPLA$_1$-Iβ1f	Glyma.18G251700	*GmPLA$_1$-Iβ1f*	LOC100817820	XM_003551664.3	XP_003551712.2	0	1	0	457	50803	8.33	0	0	0	1	0	Cytosol/Chloroplast[a]
PLA1-I	GmPLA$_1$-Iβ1a	Glyma.09G243100	*GmPLA$_1$-Iβ1a*	LOC100801635	XM_003533517.3	XP_003533565.1	0	1	0	423	47413	9.1	0	0	0	1	0	Chloroplast/Mitochondria[a]
PLA1-I	GmPLA$_1$-Iβ1b	Glyma.18G251500	*GmPLA$_1$-Iβ1b*	LOC100816744	XM_003551662.3	XP_003551710.1	1	1	0	430	48544	9.33	0	0	0	1	0	Chloroplast/Mitochondria[a]
PLA1-I	GmPLA$_1$-Iβ1c	**Glyma.09G243000**	*GmPLA$_1$-Iβ1c*	**LOC100800549**	**XM_003533515.3**	**XP_003533563.3**	**0**	**1**	**0**	**445**	**50152**	**9.48**	**0**	**0**	**0**	**1**	**0**	**Mitochondria/Chloroplast[a]**
PLA1-I	GmPLA$_1$-Iβ1d	Glyma.18G251600	*GmPLA$_1$-Iβ1d*	LOC100817287	XM_003551663.2	XP_003551711.2	0	1	0	447	50686	9.48	0	0	0	1	0	Chloroplast
PLA1-I	GmPLA$_1$-Iβ2a	Glyma.11G036900	*GmPLA$_1$-Iβ2a*	LOC100819994	XM_003538999.3	XP_003539047.1	16	1	0	523	58515	8.9	0	0	0	1	0	Chloroplast
PLA1-I	GmPLA$_1$-Iβ2b	Glyma.01G205900	*GmPLA$_1$-Iβ2b*	LOC100806573	XM_003517357.3	XP_003517405.1	43	1	0	524	58745	8.64	0	0	0	1	0	Chloroplast
PLA1-I	GmPLA$_1$-Iβ2c	Glyma.17G145900	*GmPLA$_1$-Iβ2c*	LOC100819591	XM_003549891.3	XP_003549939.1	1	1	0	528	58832	9.23	0	0	0	1	0	Mitochondria/Chloroplast[a]
PLA1-I	GmPLA$_1$-Iβ2d	Glyma.05G064200	*GmPLA$_1$-Iβ2d*	LOC100778514	XM_003524048.3	XP_003524096.1	12	1	0	540	60241	9.33	0	0	0	1	0	Chloroplast
PLA1-II	**GmPLA$_1$-IIγa**	**Glyma.13G231100**	***GmPLA$_1$-IIγa***	**LOC100815423**	**XM_003541661.3**	**XP_003541709.1**	**2**	**2**	**1**	**421**	**47583**	**9.06**	**0**	**0**	**0**	**1**	**0**	**Chloroplast/Mitochondria[a]**
PLA1-II	GmPLA$_1$-IIγb	Glyma.15G081400	*GmPLA$_1$-IIγb*	LOC100781609	XM_003547116.3	XP_003547164.2	0	2	1	425	47943	9.24	0	0	0	1	0	Cytosol/Secretory pathway[a]
PLA1-II	GmPLA$_1$-IIγc	Glyma.07G204800	*GmPLA$_1$-IIγc*	LOC100782473	XM_003528432.3	XP_003528480.1	0	2	1	402	44585	6.38	0	0	0	1	0	Mitochondria
PLA1-II	GmPLA$_1$-IIαa	Glyma.07G204900	*GmPLA$_1$-IIαa*	LOC100783553	XM_003528434.3	XP_003528482.1	27	2	1	408	45952	7.69	0	0	0	1	0	Peroxisome/Other[a]
PLA1-II	GmPLA$_1$-IIαb	Glyma.07G205000	*GmPLA$_1$-IIαb*	LOC100784086	XM_003528435.3	XP_003528483.1	0	2	1	366	41404	6.02	0	0	0	1	0	Chloroplast/Other[a]
PLA1-III	**GmPLA$_1$-III**	**Glyma.08G100400**	***GmPLA$_1$-III***	**LOC100805331**	**XM_003532660.3**	**XP_003532708.1**	**1**	**1**	**0**	**497**	**56964**	**6.85**	**0**	**0**	**0**	**1**	**0**	**Chloroplast/Mitochondria[a]**
PA-preferring PLA1	GmPA-PLA1	Glyma.09G234500	*GmPA-PLA1*	LOC100777360	XM_003533480.3	XP_003533528.1	-	20	19	914	104586	5.4	0	0	0	0	1	Nucleus/Other[a]
sPLA	GmsPLA$_2$-βI	Glyma.01G004000	*GmsPLA$_2$-βI*	LOC100527431	NM_001249057.1	NP_001235986.1	5	3	2	138	14799	7.44	-	-	-	-	-	Extracellular/Secretory pathway[a]
sPLA	GmsPLA$_2$-βII	Glyma.07G127900	*GmsPLA$_2$-βII*	LOC100781229	NM_001254251.1	NP_001241180.1	15	3	2	138	14908	7.91	-	-	-	-	-	Extracellular/Secretory pathway[a]
sPLA	**GmsPLA$_2$-αI**	**Glyma.07G129900**	***GmsPLA$_2$-αI***	**LOC100500260**	**NM_001248551.2**	**NP_001235480.1**	**8**	**4**	**3**	**156**	**17013**	**6.77**	**-**	**-**	**-**	**-**	**-**	**Chloroplast/Secretory pathway[a]**
sPLA	GmsPLA$_2$-αII	Glyma.08G028800	*GmsPLA$_2$-αII*	LOC100787294	NM_001253213.2	NP_001240142.1	15	4	3	158	17362	7.41	-	-	-	-	-	Extracellular/Secretory pathway[a]
sPLA	GmsPLA$_2$-αIb	Glyma.01G002400	*GmsPLA$_2$-αIb*	LOC100797904	NM_001254447.2	NP_001241376.1	13	4	3	157	17138	6.26	-	-	-	-	-	Chloroplast/Secretory pathway[a]